

# On Silica Activity and Serpentinization

**B. RONALD FROST<sup>1</sup>\* AND JAMES S. BEARD<sup>2</sup>**

<sup>1</sup>DEPARTMENT OF GEOLOGY AND GEOPHYSICS, UNIVERSITY OF WYOMING, LARAMIE, WY 82072, USA

<sup>2</sup>VIRGINIA MUSEUM OF NATURAL HISTORY, 21 STARLING AVENUE, MARTINSVILLE, VA 24112, USA

**RECEIVED OCTOBER 3, 2006; ACCEPTED MARCH 29, 2007  
ADVANCE ACCESS PUBLICATION MAY 28, 2007**

*Serpentinites have the lowest silica activity of common crustal rocks. At the serpentinization front, where olivine, serpentine, and brucite are present, silica activities (relative to quartz) are of the order of  $10^{-2.5}$  to  $10^{-5}$ , depending on the temperature. Here we argue that this low silica activity is the critical property that produces the unusual geochemical environments characteristic of serpentinization. The formation of magnetite is driven by the extraction of silica from the  $\text{Fe}_3\text{Si}_2\text{O}_5(\text{OH})_4$  component of serpentine, producing extremely reducing conditions as evinced by the rare iron alloys that partially serpentinized peridotites contain. The incongruent dissolution of diopside to form  $\text{Ca}^{2+}$ , serpentine, and silica becomes increasingly favored at lower T, producing the alkalic fluids characteristic of serpentinites. The interaction of these fluids with adjacent rocks produces rodingites, and we argue that desilication is also part of the rodingite-forming process. The low silica activity also explains the occurrence of low-silica minerals such as hydrogrossular, andradite, jadeite, diaspore, and corundum in serpentinites or rocks adjacent to serpentinites. The tendency for silica activity to decrease with decreasing temperature means that the presence of certain minerals in serpentinites can be used as indicators of the temperature of serpentinization. These include, with decreasing temperature, diopside, andradite and diaspore. Because the assemblage serpentine + brucite marks the lowest silica activity reached in most serpentinites, the presence and distribution of brucite, which commonly is a cryptic phase in serpentinites, is critical to interpreting the processes that lead to the hydration of any given serpentine.*

**KEY WORDS:** *serpentinization; serpentinites; silica activity; oxygen fugacity; rodingites; magnetization of serpentinites*

## INTRODUCTION

Serpentine has been long known to host unusual minerals such as awaruite ( $\text{FeNi}_3$ ), heazlewoodite ( $\text{Ni}_3\text{S}_2$ ), and hydrogarnet that are rarely found in any other geological environment. In addition, the fluids evolving from serpentinites are

exceptionally reduced (Abrajano *et al.*, 1988; Charlou *et al.*, 1998; Kelley *et al.*, 2001) and, with  $\text{pH} > 10$ , are some of the most alkaline fluids on Earth (Barnes & O'Neil, 1969; Barnes *et al.*, 1978). Because of the unusual geological conditions, serpentinization has long elicited interest among petrologists (Frost, 1985, and references therein). Recent discoveries of sea-floor hydrothermal vents that could have originated from serpentinization (Beard & Hopkinson, 2000; Kelley *et al.*, 2001; Charlou *et al.*, 2002), and the recognition that the reducing conditions of fluids emitted from serpentinization would be an ideal environment for the origin of life (Russell & Hall, 1997; Sleep *et al.*, 2004; Russell & Arndt, 2005) have provoked an increase in studies on the importance of serpentinization to sea-floor processes (Schroeder *et al.*, 2002; Kelley *et al.*, 2005; Bach *et al.*, 2006).

The authors recently had the good fortune to participate in the Integrated Ocean Drilling Program (IODP) expeditions 304 and 305, which drilled the Atlantis Massif at 20°N on the Mid-Atlantic Ridge. The >1 km of core recovered was mostly gabbro, but the core also contained significant amounts of olivine-rich troctolite. Millimeter-scale serpentine veins locally cut the troctolite and where the veins intersect plagioclase the plagioclase was altered to prehnite and grossular, assemblages common in rodingites. Because plagioclase is the only Ca-bearing phase in the troctolites, we concluded that these micro-rodingites must have formed by desilication of the plagioclase rather than the addition of CaO from outside the system (Frost *et al.*, 2005). This insight prompted us to recognize the important role that silica activity plays in serpentinization.

## SERPENTINITES AND SILICA ACTIVITY

### A note on databases and standard states

Most reactions were calculated using the THERMOCALC database of Holland & Powell (1998). Because greenalite

© 2007 The Author(s)

This is an Open Access article distributed under the terms of the Creative Commons Attribution Non-Commercial License (<http://creativecommons.org/licenses/by-nc/2.0/uk/>) which permits unrestricted non-commercial use, distribution, and reproduction in any medium, provided the original work is properly cited.

\*Corresponding author. Telephone: 307-766-4290. Fax: 307-766-6679. E-mail: rfrost@uwoyo.edu

and saponite are not in the Holland and Powell database, reactions involving these phases were calculated at 1 bar using Geochemist's Workbench<sup>®</sup> (Bethke, 2005), which incorporates a modified version of the SUPCRT92 database (Johnson *et al.*, 1992). In these calculations we used *thermo.com.v8.6+*, the updated version of the thermo database. Activities were calculated using a modified Debye–Hückel equation (Bethke, 2005). Databases were not mixed: each diagram was calculated from a single database. In any event, in the serpentinite system the huge free energy changes in the reactions swamp the small uncertainties in the thermodynamic values of the individual phases. Indeed, test calculations done using the two databases yield essentially equivalent results.

We used chrysotile as our serpentine mineral, despite the fact that Evans (2004) recently noted that it is likely to form metastably. We do this because adequate thermodynamic data are not available for lizardite, the stable form of low-*T* serpentine, and because antigorite, the high-*T* temperature form of serpentine, is only rarely seen to have formed by direct hydration of a peridotite. In actuality, the choice of which serpentine polymorph to use makes little difference; the free energy change involved in the hydration reactions studied vastly overwhelms the small energy differences between lizardite, chrysotile and antigorite.

Although mantle peridotites generally contain olivine with about 10 mol % fayalite component, we calculated most of our diagrams for the pure Mg-system. We chose to do this because our calculations showed that between the pure Mg-system and the compositions typically found in metaperidotites the location of the silica buffers is relatively insensitive to the small change in  $\mu_{\text{FeMg-1}}$ . For example, calculations using the QUILF program of Andersen *et al.* (1993) indicate that for the olivine–Opx silica buffer [equilibrium (1)], there is only a difference of 0.02 log units in silica activity between the pure system and the system where  $X_{\text{Mg}}^{\text{Ol}} = 0.9$  (the common value for olivine in the mantle).

We recognize two standard states for silica. When we are comparing silica activity of serpentinites with silica activity in other rocks, we use the standard state of pure quartz at *T* and *P* of interest. This variable we call  $a_{\text{SiO}_2}$  and it is a measure of the chemical potential change between the assemblage in question and pure quartz. When discussing the silica activity in systems that involve dissolution reactions we reference silica activity to the standard state of the dissolved form of pure quartz at the *T* and *P* of interest [i.e. the activity of  $\text{H}_4\text{SiO}_4$ , or  $\text{SiO}_2(\text{aqueous})$ ]. This variable we call  $a_{\text{SiO}_2(\text{aq})}$ . The difference between the two terms is shown in Fig. 1, which shows the variation of  $\log a_{\text{SiO}_2}$  vs *T* for pure quartz. We can convert the  $\log a_{\text{SiO}_2}$  for a given reaction to  $\log a_{\text{SiO}_2(\text{aq})}$  by simply adding the value of  $\log a_{\text{SiO}_2(\text{aq})}$  for

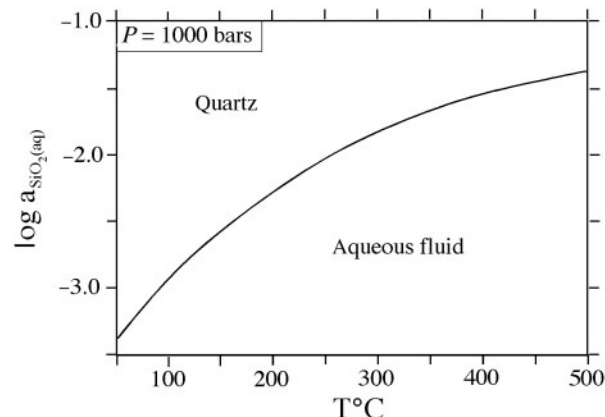


Fig. 1.  $T$ – $\log a_{\text{SiO}_2(\text{aq})}$  diagram showing the solubility of quartz at a pressure of 1 kbar.

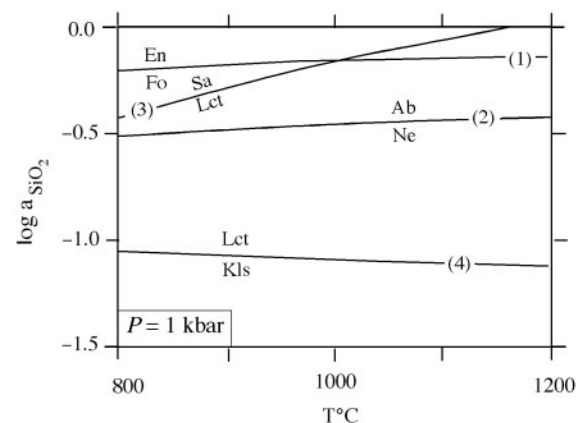


Fig. 2.  $T$ – $\log a_{\text{SiO}_2(\text{aq})}$  diagram showing a number of common silica buffers in igneous rocks at a pressure of 1 kbar. Numbered reactions are those in Table 2.

quartz at the *T* and *P* of interest. To accommodate the huge temperature dependence of the oxygen buffers, we normalize the oxygen fugacity to a common buffer. In most calculations we normalize it to the fayalite–magnetite–quartz (FMQ) buffer and call the variable  $\Delta \log f_{\text{O}_2}$ , which is defined as the deviation from the FMQ buffer. In one calculation we normalize it to the iron–magnetite (IM) buffer and in this instance we refer to the oxygen fugacity as IM, IM + 2 or IM + 4; that is, to the IM buffer or to the IM buffer + 2 or 4 log units of oxygen fugacity, respectively.

### Silica activity in igneous rocks

Silica activity has long been used in the classification of igneous rocks (Carmichael *et al.*, 1974), even though it has rarely been assigned a numerical value. Thus, it is helpful to compare the silica activity in serpentinites with that of the well-known igneous buffers (Fig. 2). With decreasing silica activity the normative minerals in igneous rocks are

Table 1: Mineral compositions and abbreviations

Formula	Phase	Abbreviation
AlO(OH)	diaspore	Dsp
CaAl <sub>2</sub> Si <sub>2</sub> O <sub>8</sub>	anorthite	An
Ca <sub>3</sub> Al <sub>2</sub> Si <sub>3</sub> O <sub>12</sub>	grossular	Grs
Ca <sub>3</sub> Al <sub>2</sub> Si <sub>2</sub> O <sub>8</sub> (SiO <sub>4</sub> ) <sub>(1-x)</sub> (OH) <sub>4x</sub>	hydrogrossular	Hgr
Ca <sub>3</sub> Fe <sub>2</sub> Si <sub>3</sub> O <sub>12</sub>	andradite	Adr
Ca(Mg,Fe)Si <sub>2</sub> O <sub>6</sub>	clinopyroxene (diopside, hedenbergite)	Cpx (Di,Hd)
Ca <sub>2</sub> Mg <sub>5</sub> Si <sub>8</sub> O <sub>22</sub> (OH) <sub>2</sub>	tremolite	Tr
CaMg <sub>18</sub> Al <sub>2</sub> Si <sub>22</sub> O <sub>60</sub> (OH) <sub>12</sub>	Ca-saponite	Ca-Sap
CaO	portlandite	Por
Fe <sup>°</sup>	native iron	I
FeNi <sub>3</sub>	awaruite	Aw
Fe <sub>3</sub> O <sub>4</sub>	magnetite	Mag
KAlSi <sub>3</sub> O <sub>8</sub>	K-feldspar	Ksp, Sa
KAlSi <sub>2</sub> O <sub>6</sub>	leucite	Lct
KAlSiO <sub>4</sub>	kalsilite	Kls
(Mg,Fe) <sub>2</sub> SiO <sub>4</sub>	olivine (forsterite, fayalite)	Ol (Fo, Fay)
(Mg,Fe)SiO <sub>3</sub>	orthopyroxene (enstatite, ferrosilite)	Opx (En, Fs)
Mg <sub>7</sub> Si <sub>8</sub> O <sub>22</sub> (OH) <sub>2</sub>	anthophyllite	Ath
Mg <sub>3</sub> Si <sub>4</sub> O <sub>10</sub> (OH) <sub>2</sub>	talc	Tlc
(Mg,Fe) <sub>3</sub> Si <sub>2</sub> O <sub>5</sub> (OH) <sub>4</sub>	serpentine, Fe-serpentine	Srp, Fe-Srp
(Mg,Fe)(OH) <sub>2</sub>	brucite, amakinite	Brc, Fe-Brc
Mg <sub>5</sub> Al <sub>2</sub> Si <sub>3</sub> O <sub>10</sub> (OH) <sub>8</sub>	chlorite (clinochlore)	Chl
Mg <sub>19</sub> Al <sub>2</sub> Si <sub>22</sub> O <sub>60</sub> (OH) <sub>12</sub>	Mg-saponite	Mg-Sap
NaAlSi <sub>3</sub> O <sub>8</sub>	albite	Ab
NaAlSi <sub>2</sub> O <sub>6</sub>	jadeite	Jd
NaAlSi <sub>2</sub> O <sub>6</sub> ·H <sub>2</sub> O	analcite	Acm
NaAlSiO <sub>4</sub>	nepheline	Ne
SiO <sub>2</sub>	quartz	Q
SiO <sub>2</sub> (aq)	aqueous silica	
Common buffers		
Assemblage	Abbreviation	
Fay-Mag-Q	FMQ	
I-Mag	IM	
Q-Fay-I	QFI	

hypersthene, olivine, nepheline and leucite, and kalsilite (see Table 1 for compositions and abbreviations of phases in this paper). The reactions that relate these phases are given in Table 2. Because peridotitic rocks do not contain feldspars or feldspathoids, the reactions involving nepheline, leucite, and kalsilite are provided in Fig. 2 merely for reference.

Table 2: Silica-dependent equilibria in igneous systems

Equilibrium	Number
2 En = Fo + SiO <sub>2</sub>	(1)
Ab = Ne + 2 SiO <sub>2</sub>	(2)
Ksp = Lct + SiO <sub>2</sub>	(3)
Lct = Kls + SiO <sub>2</sub>	(4)

Reactions in this and following tables are numbered in approximate order that they appear in the figures or the text.

The reaction between olivine and orthopyroxene [reaction (1)], which can be applied to both basalts and peridotites, corresponds to the plane of critical silica saturation (Yoder & Tilley, 1962). At silica activities above those of reaction (1) a basalt is a hypersthene-normative tholeiite, whereas at lower silica activities it is nepheline-normative and will be classified as an alkali basalt. Because fayalitic olivine can coexist with quartz, equilibrium (1) is dependent on  $\mu_{\text{FeMg-1}}$  as well as  $T$  and  $P$ . However, as noted above, because the small changes in  $\mu_{\text{FeMg-1}}$  between the pure system and the composition of minerals in the typical mantle have only a minimum effect on the location of equation (1) (and other silica buffers in the ultramafic system) we use the pure Mg system in all the calculations in this paper.

Figure 2 indicates that most igneous rocks have crystallized at silica activities above  $10^{-0.5}$ ; only in the rarely occurring kalsilite-bearing rocks are silica activities lower than  $10^{-1}$ . These silica buffers are moderately dependent on pressure; increasing pressure from 1 to 10 kbar decreases silica activity for the olivine–Opx assemblage by 0.2 log units and increases the silica activity for the upper stability of kalsilite by 0.5 log units.

### Silica activity in serpentinites and metaperidotites

The silica activity for metaperidotites falls from that defined by the olivine–Opx assemblage to lower values with decreasing temperature and increasing hydration of the assemblage (Table 3, Fig. 3). In assemblages containing anthophyllite and talc, two relatively silica-rich minerals, this trend is not particularly steep, but it becomes dramatic in assemblages where serpentine is in equilibrium with olivine or brucite. In an equilibrium assemblage of olivine, serpentine and brucite, the silica activity is nearly  $10^{-2.5}$ . These values are far lower than those in igneous rocks (even when the igneous silica buffers are extended to low temperatures), making serpentinites among the most silica-deprived rocks on Earth.

Table 3: Silica-dependent equilibria in metaperidotites

Equilibrium	Number
2 En = Fo + SiO <sub>2</sub>	(1)
2 Ath = 7 Fo + 9 SiO <sub>2</sub> + 2 H <sub>2</sub> O	(5)
2 Tlc = 3 Fo + 5 SiO <sub>2</sub> + 2 H <sub>2</sub> O	(6)
Srp + 2 SiO <sub>2</sub> = Tlc + H <sub>2</sub> O	(7)
2 Srp = 3 Fo + SiO <sub>2</sub> + 4 H <sub>2</sub> O	(8)
Srp + H <sub>2</sub> O = 3 Brc + 2 SiO <sub>2</sub>	(9)
Ath + Fo = 9 En + H <sub>2</sub> O	(10)
9 Tlc + 4 Fo = 5 Ath + 2 H <sub>2</sub> O	(11)
5 Srp = 6 Fo + Tlc + 9 H <sub>2</sub> O	(12)
Srp + Brc = 2 Fo + 3 H <sub>2</sub> O	(13)
Fo + H <sub>2</sub> O = 2 Brc + SiO <sub>2</sub>	(14)
Fo + 4 Brc + 3 SiO <sub>2</sub> = 2 Srp	(15)
3 Opx + SiO <sub>2</sub> + H <sub>2</sub> O = Tlc	(16)
3 Opx + 2 H <sub>2</sub> O = Srp + SiO <sub>2</sub>	(17)
6 Opx + 3 H <sub>2</sub> O = Srp + Tlc	(18)
3 Opx + 3 SiO <sub>2</sub> + Srp = 2 Tlc	(19)

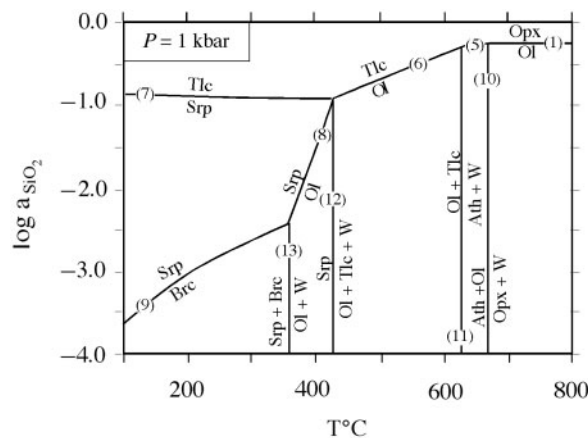
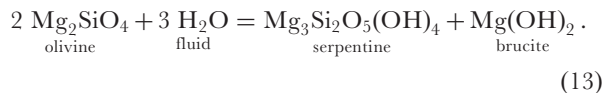


**Fig. 3.**  $T$ - $\log a_{\text{SiO}_2(\text{aq})}$  diagram showing silica buffers in metaperidotites at a pressure of 1 kbar. Numbered reactions are those in Table 3.

The hydration of olivine is usually described by the model reaction



In few environments does serpentinization occur at  $P_{\text{H}_2\text{O}} = P_{\text{total}}$  [i.e. along reaction (13) in Fig. 3]. In most occurrences the reaction of olivine to serpentine occurs at temperatures that are far below those where serpentinization would occur under water saturation. In such environments, serpentinization is

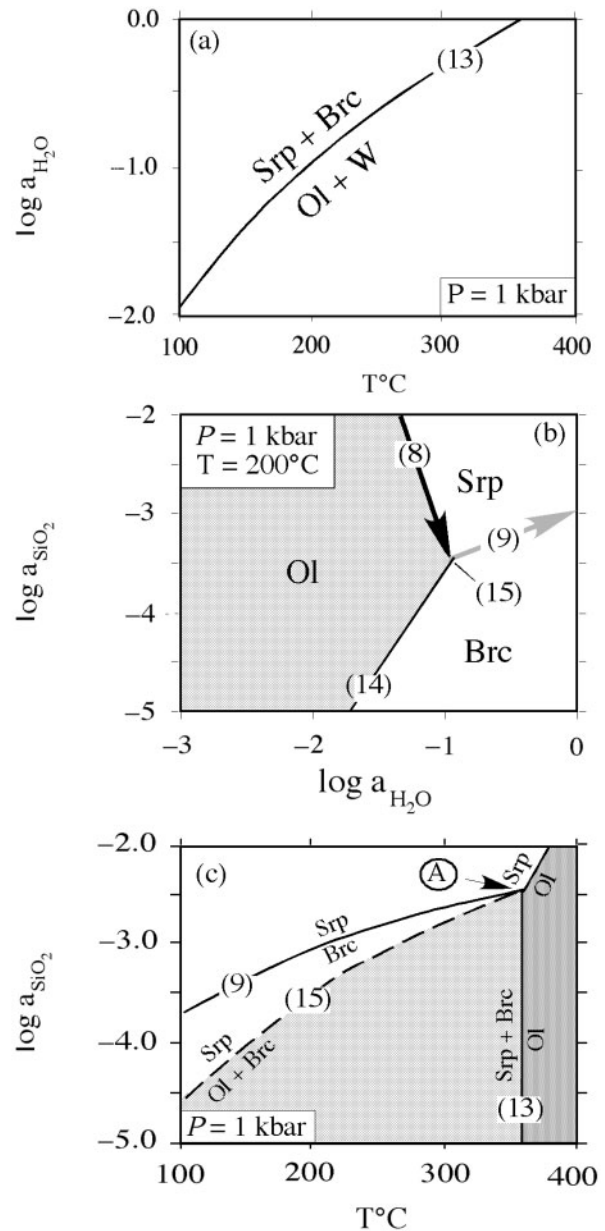
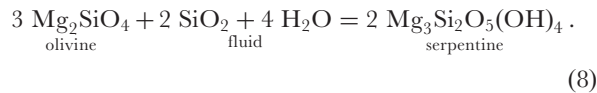


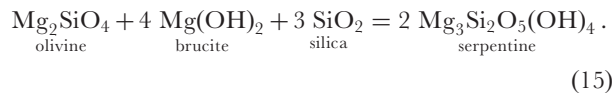
**Fig. 4.** The behavior of silica activity during serpentinization of olivine. (a) Diagram showing how  $\log a_{\text{H}_2\text{O}}$  required to serpentinize olivine varies as a function of temperature. (b) Plot showing how silica activity and water activity co-vary during serpentinization. (c)  $T$ - $\log a_{\text{SiO}_2}$  plot showing the relation between the stable silica buffers in serpentinites and the silica activity attained during low- $T$  serpentinization of metastable olivine (dashed line). This is the trace of the invariant point A with decreasing water activity, as modeled by reaction (15).

controlled by the access of water into the rock. Because of the large amount of water necessary to produce serpentinization, the water activity for reaction (13) falls dramatically with falling  $T$  (Fig. 4a). The effect of variations in  $a_{\text{H}_2\text{O}}$  on the silica activity of

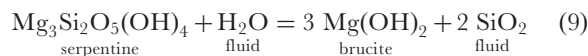
serpentinization can be shown on an isobaric, isothermal  $\log a_{\text{SiO}_2} - \log a_{\text{H}_2\text{O}}$  diagram (Fig. 4b). Serpentinization probably begins by conversion of olivine by the reaction



Progress along reaction (8) would rapidly drop silica activity in the fluid to the point where brucite would be stable and reaction (13) can begin (although at a temperature that may be considerably lower than it would be in a water-saturated system). At this point the water-conserved equilibrium relating the three solid phases would be the isobaric, isothermal, invariant reaction



This equilibrium involves the same phases as reaction (13) only it has been written with silica as the mobile component, rather than water. Writing the reaction in this way allows us to monitor the silica activity attendant with serpentinization that occurs at temperatures below those where olivine hydrates in systems where  $P_{\text{H}_2\text{O}} = P_{\text{total}}$ . The silica activity for the invariant assemblage olivine-serpentine-brucite lies below that where serpentine + brucite + water coexist. Only after olivine is completely eliminated from the assemblage does the hydration of serpentine to brucite and silica, according to the reaction



drive silica activity to higher values.

The silica activity that accompanies low- $T$  serpentinization can be monitored from reaction (15) (Fig. 4c). Reaction (15) is shown as a dashed line in Fig. 4c to emphasize that curve is not valid for  $P_{\text{H}_2\text{O}} = P_{\text{total}}$ , as are the other curves in Fig. 4c, but that it is the trace followed by invariant point (A) with decreasing water activity. At all temperatures, however, the serpentinization reaction [reaction (13)], remains the same. Figure 4c shows that silica activity during low- $T$  serpentinization may be more than two log units lower than it would be at temperatures where brucite + serpentine + pure water occur in equilibrium.

Of course, in most peridotites, orthopyroxene will be involved in the hydration reactions as well as olivine. In the hydration of an Opx-bearing rock the initial reaction will be to form talc by the reaction

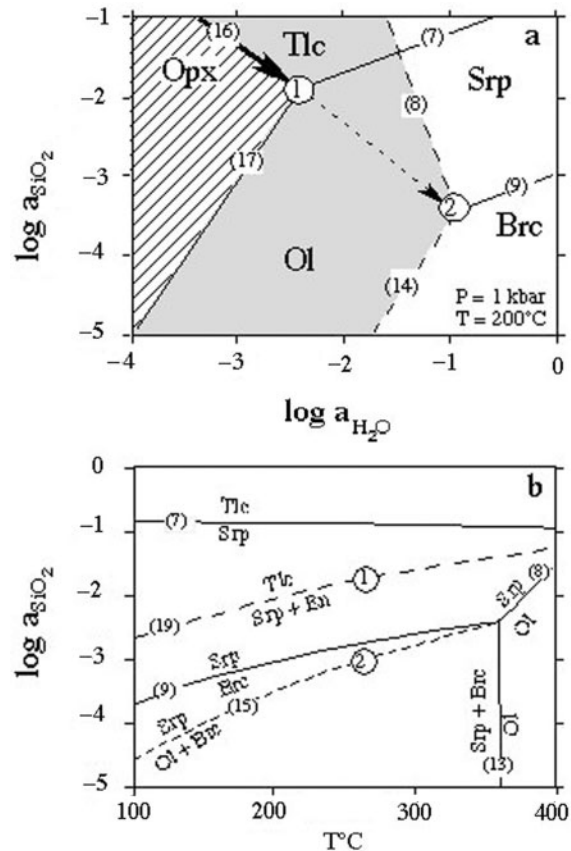
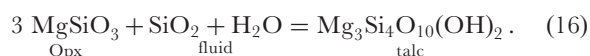
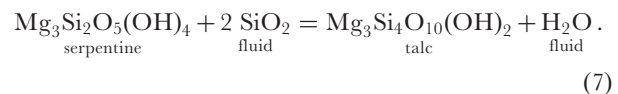
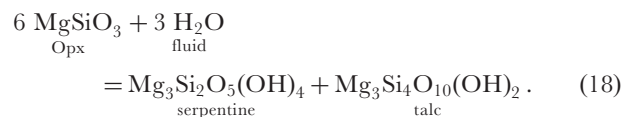


**Fig. 5.** (a)  $\log a_{\text{SiO}_2} - \log a_{\text{H}_2\text{O}}$  and (b)  $T - \log a_{\text{SiO}_2}$  diagrams showing the processes encountered in the serpentinization of Opx-bearing peridotite at water activities well below unity. Initial influx of fluids will produce serpentinization reactions involving olivine + enstatite (point 1). When Opx is depleted from the rock, silica activity will fall until it is defined by the equilibrium between olivine, serpentine, and brucite (point 2). Water activity will still be less than unity. Once olivine has been depleted from the rock silica activity will rise to values determined by the serpentine-brucite buffer (point 3). Water activity may also rise to unity.

Only a small amount of progress along this reaction will deplete silica from the fluid until the reaction meets the talc-serpentine silica buffer (point 1, Fig. 5a),



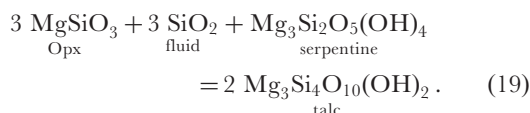
At this point the isobaric, isothermal invariant reaction becomes



If the Opx occurred in an orthopyroxenite, hydration by reaction (18) would lead to the production of equal moles of serpentine and talc. If the Opx was in a peridotite

where olivine was also being hydrated (point 2, Fig. 5a), silica will tend to move from the talc-bearing portions of the rock (area 1) to the brucite-bearing portions, eliminating talc from the assemblage (dashed arrow in Fig. 5a).

To calculate the temperature dependence of the silica activity at the invariant point in Fig. 5a we can write a reaction for the assemblage Opx–Srp–Tlc using silica as a mobile component:



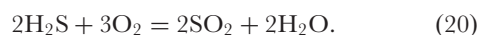
The trajectory followed by this invariant point applies only to situations where  $P_{\text{H}_2\text{O}} = P_{\text{total}}$  because the water activity necessary to destabilize the assemblage Opx–serpentine–talc decreases with decreasing temperature. As a result, this curve is shown with dashed lines in Fig. 5b.

Figure 5a and b shows that a gradient in silica activity of a log unit or more could be present between serpentinite formed from Opx (point 1 in Fig. 5a and b) and that from surrounding olivine (point 2 in Fig. 5a and b). The extent of this gradient will depend upon the relative rates of the reactions that hydrate olivine and Opx and on the efficiency of fluid flow through the rock. The fact that talc may form rims between Opx and serpentine in bastites (Viti *et al.*, 2005) suggests that in some serpentinites a large silica activity gradient may be present on a millimeter scale.

## OXYGEN AND SULFUR FUGACITIES

### Low oxygen and sulfur fugacities

One of the most distinctive features of serpentinite is its extremely low oxygen fugacity, as indicated by the fact that serpentinites are one of the few crustal environments where iron alloys occur (Frost, 1985). The occurrence of iron and nickel as metallic alloys, rather than in sulfides indicates that serpentinites also have very low sulfur fugacity. As noted by Frost (1985), sulfur fugacity in metamorphic rocks is a function of oxygen fugacity because sulfur is present dominantly as  $\text{H}_2\text{S}$  or  $\text{SO}_2$ , rather than  $\text{S}_2$ . The fugacities of  $\text{H}_2\text{S}$  and  $\text{SO}_2$  are related by the reaction (Table 4)



The oxygen fugacity at which the partial pressures of  $\text{H}_2\text{S}$  and  $\text{SO}_2$  are equal is called the sulfate–sulfide fence. At the temperatures of serpentinitization the sulfide–sulfate fence lies well above the oxygen fugacity of the FMQ buffer (see Frost, 1985), and, hence, far above the oxygen fugacities ambient in serpentinites. At oxygen fugacities

Table 4: Oxygen-dependent equilibria in metaperidotites

Equilibrium	Number
$2 \text{ H}_2\text{S} + 3 \text{ O}_2 = 2 \text{ SO}_2 + 2 \text{ H}_2\text{O}$	(20)
$\text{S}_2 + 2 \text{ H}_2\text{O} = 2 \text{ H}_2\text{S} + \text{O}_2$	(21)
$\text{Ol} (\text{Fo}_{90}\text{Fay}_{10}) + 1.3 \text{ H}_2\text{O} + 0.034 \text{ O}_2$ $+ 0.067 \text{ Mag} + 0.5 \text{ Srp} + 0.3 \text{ Brc}$	(22)
$2 \text{ Fe-Srp} + \text{O}_2 = 2 \text{ Mag} + 4 \text{ SiO}_2 + 4 \text{ H}_2\text{O}$	(23)
$2 \text{ H}_2\text{O} = 2 \text{ H}_2 + \text{O}_2$	(24)
$\text{Mag} = 3 \text{ l} + 2 \text{ O}_2$	(25)
$4 \text{ Fe-Srp} = 3 \text{ l} + 3 \text{ Mag} + 4 \text{ SiO}_2 + 8 \text{ H}_2\text{O}$	(26)
$6 \text{ Fe}(\text{OH})_2 + \text{O}_2 = 2 \text{ Mag} + 6 \text{ H}_2\text{O}$	(27)
$2 \text{ Fe}(\text{OH})_2 = 2 \text{ l} + 2 \text{ H}_2\text{O} + \text{O}_2$	(28)
$2 \text{ Fe-Srp} = 6 \text{ l} + 4 \text{ SiO}_2 + 4 \text{ H}_2\text{O} + 3 \text{ O}_2$	(29)

below the sulfate–sulfide fence sulfur fugacity is controlled by the reaction



Reaction (21) clearly indicates that, as oxygen fugacity falls from the values defined by the sulfide–sulfate fence, progressively more sulfur will be driven from the sulfides into the fluid phase. This explains why fluid inclusions from some serpentinites contain measurable amounts of  $\text{H}_2\text{S}$ , even though the rock itself may contain awaruite (Peretti *et al.*, 1992).

Because of reaction (21), sulfides are a sensitive monitor of oxygen fugacity in serpentinites. As oxygen fugacity falls, the sulfide minerals stable with magnetite become increasingly poorer in sulfur relative to metal. With decreasing oxygen fugacity in serpentinites, the stable sulfide ranges from millerite ( $\text{NiS}$ ) to pentlandite ( $(\text{FeNi})_9\text{S}_8$ ) to heazlewoodite ( $\text{Ni}_3\text{S}_2$ ) (Frost, 1985). The sulfur-rich sulfides polydymite ( $\text{Ni}_3\text{S}_4$ ) and vaesite ( $\text{NiS}_2$ ) are found only in relatively oxidizing, carbonate-bearing serpentinites (Eckstrand, 1975). Although pentlandite is common in many mafic and ultramafic rock types, heazlewoodite is found only in serpentinites (Ramdohr, 1968).

Because the low sulfur activity associated with serpentinitization destabilizes sulfides, many metals are liberated from serpentinites. They are deposited in relatively more oxidized country rocks, where the increase in oxygen fugacity drives sulfur out of  $\text{H}_2\text{S}$  and back into the sulfide phases (Frost, 1985). Metals that have been concentrated adjacent to serpentinites include Ni, Cu, Co and Ag (Groves & Keays, 1979; Leblanc & Lbouabi, 1988).

During serpentinitization some of the iron in the original peridotite is driven into magnetite, making serpentinites a possible source of magnetic anomalies (Coleman, 1971; Shive *et al.*, 1988). A plot of magnetic susceptibility, which

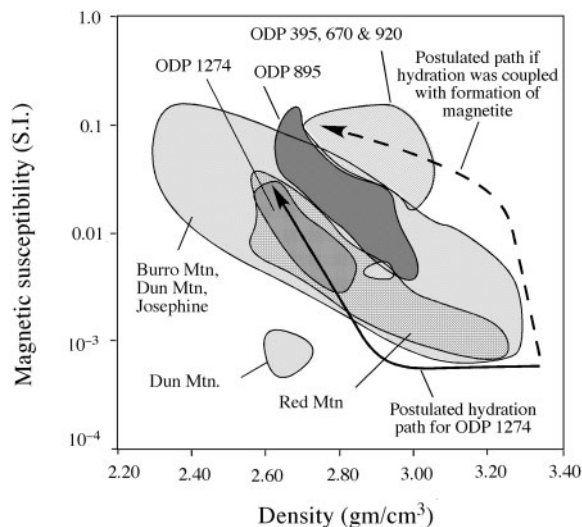
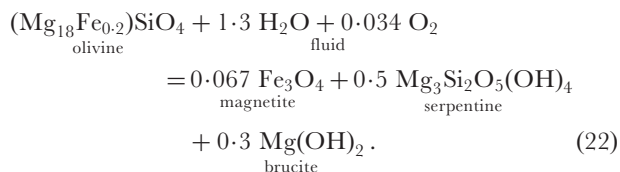


**Fig. 6.** Plot of magnetic susceptibility against density for a number of partially serpentinized serpentinites. Three samples with low density and low magnetic susceptibility from Dun Mountain form a distinct outlier. Dashed line is the path followed during serpentinization if the formation of magnetite were directly tied to hydration of olivine and pyroxene (Toft *et al.*, 1990). Continuous line is the path inferred for hydration of peridotites at ODP site 1274 (Bach *et al.*, 2006). Data are from Toft *et al.* (1990), Oufi *et al.* (2002) and Bach *et al.* (2006).

is a function of the abundance of magnetite, against density, which is a monitor of the degree of serpentinization, is a commonly used diagram from which to infer the nature of the magnetite-forming reactions in serpentinites (Toft *et al.*, 1990; Oufi *et al.*, 2002; Bach *et al.*, 2006; Fig. 6). Three things are evident from this figure. First, the path followed by hydration of peridotites does not follow the path one would predict if the formation of magnetite were directly tied to a serpentinization reaction (dashed line). A reaction that directly ties magnetite formation with serpentinization would be something like:



It does not matter what stoichiometry one uses in a model reaction such as reaction (22) [Toft *et al.* (1990) listed more than 20], progress along these reactions follows a path similar to that shown as the dashed line in Fig. 6. Early formation of magnetite will drive the susceptibility up by several orders of magnitude without a large change in density; only late in the hydration process does density decrease. For this reason, Toft *et al.* (1990) concluded that hydration of peridotite was decoupled from the formation of magnetite.

Another important conclusion that can be derived from Fig. 6 is that each occurrence of peridotite appears to

follow its own trend. Some, such as Burro Mountains, Dun Mountain, and Josephine tend to form linear trends that originate at the density and susceptibility of fresh peridotite. Others, such as Red Mountain, Ocean Drilling Program (ODP) 1274 and ODP 895, have either curvilinear trends that originate at the conditions of fresh olivine or linear trends that reach low susceptibility at densities that are considerably lower than those of fresh peridotite. Bach *et al.* (2006) postulated that these relations indicate that the formation of magnetite in peridotites commences only after a significant amount of hydration has taken place.

Another consideration in the formation of magnetite is the fact that the FeO content of serpentine from peridotites is variable. Serpentine in incipiently serpentinized peridotites tends to be more iron-rich (with  $X_{\text{Fe}} \sim 0.10$ , approximately that of the primary olivine), whereas in the highly serpentinized peridotites  $X_{\text{Fe}}^{\text{Srp}} = 0.05\text{--}0.03$  (Oufi *et al.*, 2002). A similar relation was observed by Bach *et al.* (2006), who reported that mesh pseudomorphs after olivine contain serpentine and rather Fe-rich brucite without magnetite, whereas the cores of the same meshes contain serpentine, Mg-rich brucite, and magnetite. Two other key points about magnetite and serpentine composition are that magnetite is absent in bastites (serpentine pseudomorphs after Opx) and that the serpentine in the bastites generally has similar  $X_{\text{Fe}}$  to the Opx that they have replaced (Le Gleuher *et al.*, 1990; Viti *et al.*, 2005; Bach *et al.*, 2006).

It is evident from the observations of Oufi *et al.* (2002) and Bach *et al.* (2006) that olivine hydrates by at least two reactions. In one it forms relatively iron-rich serpentine and brucite, whereas in the other it forms magnetite along with relatively magnesian serpentine and brucite. Figure 7a shows a possible explanation of how this might work. In the previous discussion we have treated serpentinization reactions as if they dealt solely with the magnesian end-members. This is reasonable because peridotites have  $X_{\text{Mg}} \sim 0.9$  and the effect of this small amount of FeO on the phase relations is minimal. Of course, we cannot continue to do this when discussing the role of magnetite, as magnetite is formed from the Fe dissolved into the silicates. In Fig. 7a we show the major silica-dependent reactions in serpentinites [reactions (7) and (9); Table 3] as reaction loops. The loops are based on the following observations. Talc is always more magnesian than serpentine; for example, when  $X_{\text{Mg}}^{\text{serpentine}} = 0.9$ ,  $X_{\text{Mg}}^{\text{talc}} = 0.975$  (Trommsdorff & Evans, 1972). The relatively Fe-rich serpentine formed from olivine may have  $X_{\text{Mg}} = 0.9$  (Oufi *et al.*, 2002). The Fe-rich brucite formed in this reaction is poorly constrained but it may be as high as  $X_{\text{Mg}} = 0.75$  (Bach *et al.*, 2006). The magnesian serpentine that occurs with magnetite has  $X_{\text{Mg}} = 0.95$  and it occurs with a brucite with  $X_{\text{Mg}} = 0.90$  (Bach *et al.*, 2006).

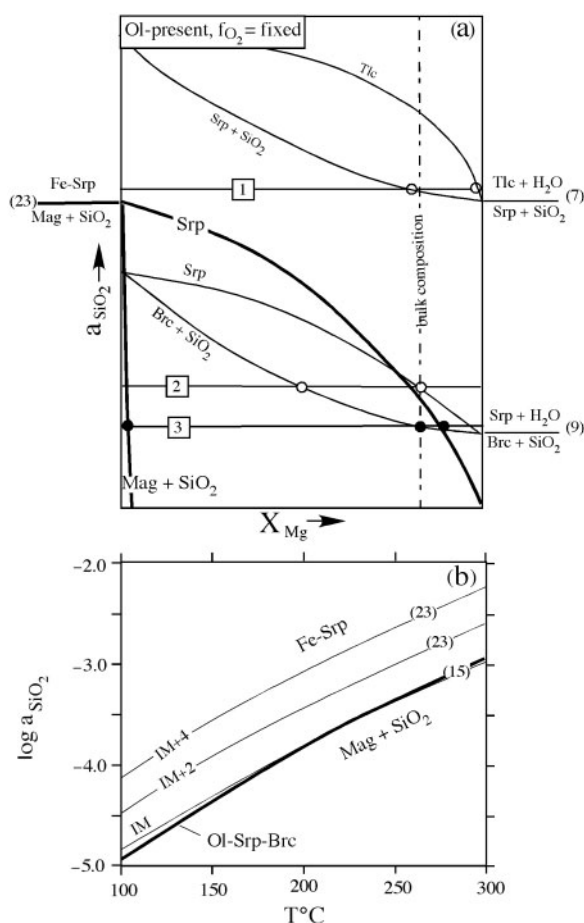
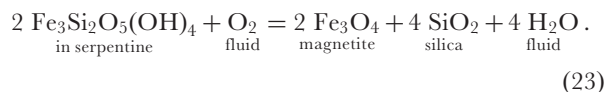


**Fig. 7.** Figures showing the relationships governing the formation of magnetite during serpentinization. (a)  $X_{Mg}$ – $\log a_{SiO_2}$  diagram showing possible relationship between the brucite–serpentine and serpentine–talc–silica buffers (with water activity controlled by the presence of olivine and Opx, respectively) (fine lines) and the oxidation of Fe-serpentine to Mag + silica (bold lines). Numbers in boxes give possible silica activity values for (1) Opx–serpentine–talc, (2) olivine–serpentine–brucite with a slightly elevated imposed silica activity, and (3) olivine–serpentine–brucite where the silica activity is internally controlled. (b) Calculated location of the serpentine–brucite buffer and the reaction Fe-serpentine = magnetite + silica for a water activity controlled by the presence of olivine and oxygen fugacities of the IM buffer and IM + 2 and IM + 4.

A third reaction on this diagram, which is shown as a bold line, is the oxidation of Fe-serpentine to produce magnetite and silica:



Because we cannot write a reaction producing magnetite using only magnesian end-members, the loop for reaction (23) does not close on the right side of Fig. 7a; instead it becomes asymptotic. Constraints on the location of the magnetite limb of this loop come from Evans & Frost (1975), who showed that in serpentinites  $X_{Mg}^{\text{magnetite}} = 0.02$ .

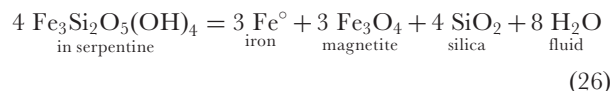
Our explanation of magnetite-absent and magnetite-present olivine hydration reactions is as follows. In a rock where silica activity is relatively high, either through serpentinization of adjacent Opx [silica activity conditions (1) in Fig. 7a] or through external supply of silica, olivine will hydrate under conditions where magnetite is not stable [silica activity conditions (2) in Fig. 7a]. Consequently, olivine will hydrate to ‘iron-rich’ serpentine and ‘iron-rich’ brucite (open circles on Fig. 7a). It should be noted that, if silica activity is high enough and there is sufficient flux of silica in the fluid, olivine may hydrate directly to serpentine by reaction (8) (Table 3), without the formation of brucite. If Opx is consumed from the rock, or if there is limited communication between Opx-bearing and olivine-bearing portions of the rock, olivine hydration will occur at lower silica activities [silica activity condition (3) in Fig. 7a] with the production of magnetite, and relatively magnesian brucite and serpentine (filled circles on Fig. 7a). It is clear that serpentinization can take place over a range of silica activities between (2) and (3) in Fig. 7a, which would explain why serpentine and brucite from partially serpentinized peridotites show a range of  $X_{Mg}$  (Oufi *et al.*, 2002; Bach *et al.*, 2006).

We cannot calculate Fig. 7a with thermodynamic rigor because we lack activity–composition relations for serpentine and brucite. However, we can use existing thermodynamic data to determine if our explanation is feasible. The relations we describe in Fig. 7a can hold only if the oxidation of serpentine to magnetite + silica [reaction (23)] in a serpentine with  $X_{Mg} = 0.9$  occurs at an oxygen fugacity and silica activity near those that attend the hydration of olivine to serpentine + brucite. Figure 7b shows the location of reaction (23) calculated for three oxygen fugacities, compared with the silica activities of the serpentine–brucite buffer when in the presence of olivine. The figure has been calculated assuming that the end-member thermodynamic properties of Fe-serpentine are similar to those of greenalite and that solution of Fe and Mg in serpentine are ideal. Figure 7b shows that the low silica activity limit for serpentine with  $X_{Fe} = 0.1$  lies close to the silica activity of the serpentine = brucite buffer in the presence of olivine, which means that the relations we describe in Fig. 7a are plausible.

### The formation and stability of iron alloys

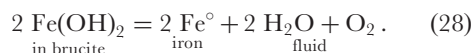
The oxygen necessary for the formation of magnetite is extracted from the decomposition of water [reaction (24)] and the hydrogen produced by this reaction makes serpentinites among the most reduced rocks on Earth. Partially serpentinized peridotites are so reducing that they commonly contain iron alloys. Awaruite (FeNi<sub>3</sub>) is the most commonly reported alloy, but

the more iron-rich, variable-composition Fe–Ni alloy, taenite (Rosetti & Zuchetti, 1998) and even pure native iron (Chamberlain *et al.*, 1965) are known. Although iron alloys are reported from serpentinites, something other than the displaced magnetite–iron buffer [reaction (25)] must form a ‘floor’ for oxygen fugacity in serpentinites. Native iron alloys are scarce in serpentinites; they usually occur as minute grains and make up an insignificant volume of the rock. Not only that, if the presence of native alloys did form the floor, then the oxygen-conserved reaction



would proceed until significant amounts of iron were extracted from the silicates.

Some other equilibrium must be operating in serpentinites that keeps the low silica activity from depleting Fe from the silicates while producing abundant magnetite and native iron. Two reasonable candidates for this are the following reactions, which cause a stability field for Fe-bearing brucite to lie between the stability field for magnetite and that for native iron:



Unfortunately the thermodynamic data available for the solution of  $\text{Fe}(\text{OH})_2$  into brucite are inadequate to calculate the phase relations between magnetite, brucite, and serpentine directly, so instead we will show inferred relations on a chemical potential diagram (Fig. 8). The key feature about the equilibria between serpentine, brucite, magnetite, and iron is that, in addition to silica activity (for serpentine) the relative stabilities of these minerals also depend on oxygen fugacity and water activity, with the stability fields for both brucite and serpentine being enhanced by increases in water activity. We know from previous discussion that at any temperature there are two conditions where the water activity (and hence the silica activity) of the assemblage serpentine + brucite is fixed; one is when water activity is unity and the other is when serpentine and brucite occur with olivine (see Fig. 4b). We have constructed Fig. 8 to explain the occurrence of alloys in the presence of relict olivine and their absence in completely serpentinitized rocks (Frost, 1985). In the presence of olivine, reduced water activity reduces the stability fields of serpentine and Fe-brucite such that awaruite is stable. When olivine is depleted from the rock, water activity increases, and the fields for both serpentine and brucite expand, and, in doing so, they consume any alloys that may have formed early in the serpentinitization process.

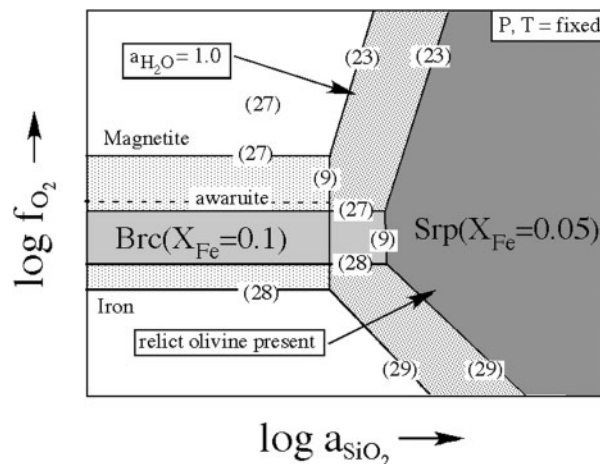
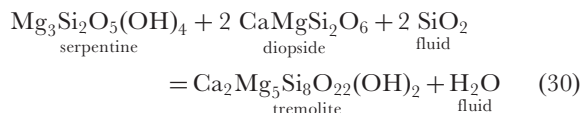


**Fig. 8.** Schematic  $\log f_{\text{O}_2} - \log a_{\text{SiO}_2}$  diagram showing the stabilities of magnetite,  $\text{Fe}(\text{OH})_2$  in brucite,  $\text{Fe}_3\text{Si}_2\text{O}_5(\text{OH})_4$  (in serpentine). Shaded fields refer to conditions where water activity is fixed by the presence of olivine (plus serpentine + brucite, magnetite, or iron). Stippled fields refer to conditions where olivine is not present and water activity is unity (or nearly so). It should be noted how the increase in water activity after the depletion of olivine from the rock will cause the stability fields of brucite and serpentine to expand, consuming the field for native metals.

## SERPENTINITES AND CALCIUM Diopside stability and fluid chemistry

Low- $T$  fluids issuing from serpentinite-hosted vents are characteristically alkaline (commonly  $\text{pH} > 10$ ) and Ca-rich (Barnes & O’Neil, 1969; Barnes *et al.*, 1978; Palandri & Reed, 2004). Both of these features are attributable to the breakdown of clinopyroxene during serpentinitization. Specifically, the absence of a stable Ca mineral requires that unbalanced dissolution of  $\text{Ca}^{2+}$  in the serpentinitizing fluid is accommodated by  $\text{OH}^-$  production (Li *et al.*, 2004; Palandri & Reed, 2004). The loss of  $\text{Ca}^{2+}$  to a fluid phase is reflected by the Ca depletion observed in many serpentinitized peridotites (Coleman, 1963; Puga *et al.*, 1999; Shervais *et al.*, 2005).

We argue here that the low silica activity of serpentinites plays a critical role in destabilizing clinopyroxene in serpentinitizing fluids (Fig. 9; Table 5). At  $a_{\text{H}_2\text{O}}$  buffered by the serpentine–brucite equilibrium [reaction (9)] diopside is unstable in fluids with the nominal composition of seawater at temperatures below about 200°C. The temperature of this reaction point decreases as  $\text{pH}$  and  $a_{\text{Ca}^{2+}}$  increase. The tremolite-forming reaction



will not occur anywhere along the serpentine–brucite silica buffer (Fig. 9a). This explains why tremolite occurs only in metaperidotites where olivine is also stable

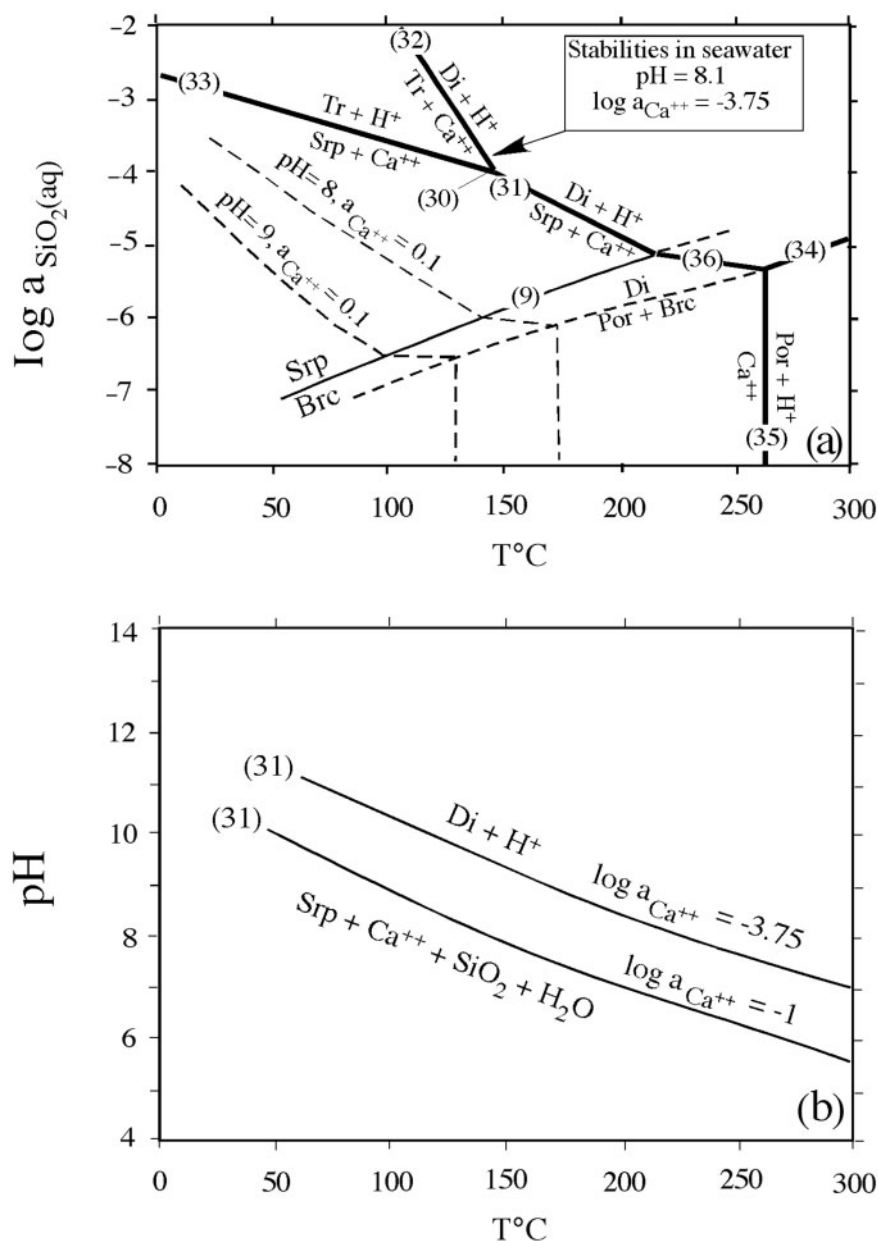
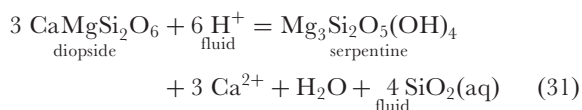


**Fig. 9.** Figures showing the stability of diopside in serpentine. (a)  $\log a_{\text{SiO}_2(\text{aq})}$ – $T$  diagram showing the stability of diopside in fluids of seawater composition (pH = 8.1,  $\log a_{\text{Ca}^{2+}} = -3.75$ ) (bold lines). Dashed lines show the effect of pH on diopside stability for constant Ca activity ( $\log a_{\text{Ca}^{2+}} = -1$ ). (b) pH vs  $T$  diagram showing how the solution of diopside on the serpentine–brucite buffer produces progressively more alkaline fluids with decreasing temperature.

(i.e. at the higher temperatures of greenschist facies; Evans, 1977). Other Ca-silicates either are unstable in the high-Mg environments of serpentinites (e.g. larnite, wollastonite) or require substantial amounts of Al (e.g. zoisite, grossular) or ferric iron (andradite). Thus the reaction



must proceed to the right with falling temperature (or falling silica activity) (Fig. 9b). This results in the serpentinization of clinopyroxene, and an increase in  $\text{Ca}^{2+}$  in the fluid along with concomitant increase in alkalinity. As temperature decreases, pH and  $\text{Ca}^{2+}$  concentration will rise (Fig. 9b). It should be noted that at temperatures in excess of 400  $^{\circ}\text{C}$ , such as seen at the Rainbow hydrothermal field, serpentinization of clinopyroxene results in fluids that are both Ca-rich and mildly acidic

Table 5: Dissolution equilibria in serpentinites

Equilibrium	Number
Srp + 2 Di + 2 SiO <sub>2</sub> = 1 Tr + H <sub>2</sub> O	(30)
3 Di + 6 H <sup>+</sup> = Srp + 3 Ca <sup>2+</sup> + H <sub>2</sub> O + 4 SiO <sub>2</sub> (aq)	(31)
5 Di + 6 H <sup>+</sup> = Tr + 3 Ca <sup>2+</sup> + 2 H <sub>2</sub> O + 2 SiO <sub>2</sub> (aq)	(32)
3 Tr + H <sub>2</sub> O + 12 H <sup>+</sup> = 5 Srp + 6 Ca <sup>2+</sup> + 14 SiO <sub>2</sub> (aq)	(33)
Di + H <sub>2</sub> O = Por + Brc + 2 SiO <sub>2</sub> (aq)	(34)
Por + 2 H <sup>+</sup> = Ca <sup>2+</sup> + H <sub>2</sub> O	(35)
Di + 2 H <sup>+</sup> = Ca <sup>2+</sup> + Brc + 2 SiO <sub>2</sub> (aq)	(36)
5 Di + 4 An + 8 H <sub>2</sub> O = 3 Grs + Chl + 6 SiO <sub>2</sub> (aq)	(37)
10 Di + 3 An + 2 H <sub>2</sub> O = 3 Grs + 2 Tr + SiO <sub>2</sub> (aq)	(38)
5 An + 2Tr + 6H <sub>2</sub> O = 3 Grs + 2 Chl + 11 SiO <sub>2</sub> (aq)	(39)
Ca <sub>3</sub> Al <sub>2</sub> Si <sub>3</sub> O <sub>12</sub> + 2x H <sub>2</sub> O = Ca <sub>3</sub> Al <sub>2</sub> Si <sub>2</sub> O <sub>8</sub> (SiO <sub>4</sub> ) <sub>(1-x)</sub> (OH) <sub>4x</sub> + xSiO <sub>2</sub> (aq)	(40)
3Adr + 9 SiO <sub>2</sub> (aq) + Mag = 9 Hd + 2 O <sub>2</sub>	(41)
3 Mag + 12 Di + 12 H <sub>2</sub> O = 4 Adr + 12 Brc + I + 12 SiO <sub>2</sub> (aq)	(42)
3 Mag + 12 Di + 8 H <sub>2</sub> O = 4 Adr + 4 Srp + I + 4 SiO <sub>2</sub> (aq)	(43)
3 Mag + 12 Di + 6 Brc + 8 H <sub>2</sub> O = 4 Adr + 6 Srp + I	(44)
3 Mag + 6 Srp + 12 H <sub>2</sub> O + 12 Ca <sup>++</sup> + 2O <sub>2</sub> = 4 Adr + 18 Brc + I + 12 H <sup>+</sup>	(45)
3 Chl + SiO <sub>2</sub> (aq) + H <sub>2</sub> O = 5 Srp + 6 Dsp	(46)
18 Sap(Mg) + 23 H <sub>2</sub> O = 19 Srp + 6 Dsp + 28 SiO <sub>2</sub> (aq)	(47)
3 Chl + 14 Srp + 29 SiO <sub>2</sub> (aq) = 3 Mg-Sap + 22 H <sub>2</sub> O	(48)
3 Mg-Sap + 2 SiO <sub>2</sub> (aq) + 5 H <sub>2</sub> O + 3 Ca <sup>2+</sup> = 3 Ca-Sap + Srp + 6 H <sup>+</sup>	(49)
13 Srp + 3 Chl + 31 SiO <sub>2</sub> (aq) + 3 Ca <sup>2+</sup> = 3 Ca-Sap + 6 H <sup>+</sup> + 17 H <sub>2</sub> O	(50)
3 Chl + 10 SiO <sub>2</sub> (aq) + 7 H <sub>2</sub> O + 9 Ca <sup>2+</sup> = 3 Grs + 5 Srp + 18 H <sup>+</sup>	(51)
6 Srp + Grs + 7 SiO <sub>2</sub> (aq) + 4 H <sup>+</sup> = Ca-Sap + 8 H <sub>2</sub> O + 2 Ca <sup>2+</sup>	(52)
Crn + 3 SiO <sub>2</sub> (aq) + 3 H <sub>2</sub> O + 3 Ca <sup>2+</sup> = Grs + 6H <sup>+</sup>	(53)
Chl + 2 H <sub>2</sub> O = 5 Brc + 2 Dsp + 3 SiO <sub>2</sub> (aq)	(54)
Crn + H <sub>2</sub> O = Dsp	(55)
5 Brc + Crn + 3 SiO <sub>2</sub> (aq) = Chl + H <sub>2</sub> O	(56)
Jd + SiO <sub>2</sub> = Ab	(57)
Acm = Jd + H <sub>2</sub> O	(58)
Acm + SiO <sub>2</sub> = Ab + H <sub>2</sub> O	(59)

(Charlou *et al.*, 2002). These fluids are forming in the presence of tremolite (Allen & Seyfried, 2003) and their acidic character is consistent with the equilibria shown in Fig. 9a and b. It should also be noted from reaction (31) that diopside-serpentine equilibria are not affected by Mg concentration in the fluid as long as serpentine is stable.

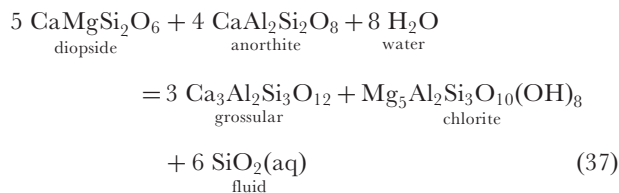
## Rodingites

Rodingites are rocks (most often basalts and gabbros, but rodingitized metasedimentary rocks and granites are also reported) that have undergone intensive

metasomatism as a consequence of the serpentinization of surrounding peridotite (Coleman, 1963, 1977; Schandl *et al.*, 1989; O'Hanley, 1996). The metasomatism is usually described in terms of Ca enrichment, and, indeed, this is observed in many or most rodingites. However, an equally common and important component of the metasomatism is Si depletion (e.g. Coleman, 1963). Many rodingites are polymetamorphic rocks that have undergone several stages of both metamorphism and metasomatism (Frost, 1975; Evans *et al.*, 1979; Schandl *et al.*, 1989; O'Hanley *et al.*, 1992; Puga *et al.*, 1999; El-Shazly & Al-Belushi, 2004; Li *et al.*, 2004). We concern ourselves here with metasomatic and metamorphic processes that are directly related to serpentinization *sensu stricto*.

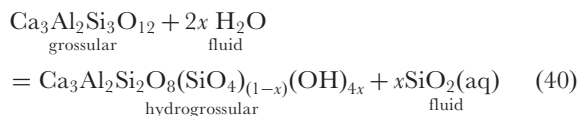
In a typical gabbroic rodingite, plagioclase is replaced by various Si-poor, usually hydrated Ca–Al silicates including grossular (and/or hydrogrossular), (clino)zoisite, prehnite, vesuvianite, wollastonite, and xonotlite [Ca<sub>6</sub>Si<sub>6</sub>O<sub>17</sub>(OH)<sub>2</sub>]. The commonest Fe–Mg silicates are usually chlorite and amphibole (especially tremolite) although serpentine minerals may also be present, especially if the protolith contained olivine. If one examines rodingite mineralogy with the assumption that Si is not fixed, it is apparent that the reaction of clinopyroxene and plagioclase in the presence of water will yield a variety of the most common rodingite assemblages (e.g. grossular-chlorite; Fig. 10a). These assemblages are the hydrated chemical equivalents of Cpx-plagioclase except that they are silica deficient. This becomes clear when silica is plotted explicitly (Fig. 10b). It is also clear from the stoichiometry of reactions (37)–(39) (Table 5). These reactions may be isochemical with respect to other components, but they are not isochemical with respect to silica.

The silica activity imposed by the brucite-serpentine buffer oversteps the rodingite reaction:



and strongly favors the Gro + Chl assemblage (Fig. 10c). At low *T* the equivalent tremolite-forming reaction [reaction (38)] is even further overstepped (Fig. 10c).

Hydrogrossular, a mineral that is virtually characteristic of rodingites and serpentinites and found in few other geological environments, is related to grossular by the reaction



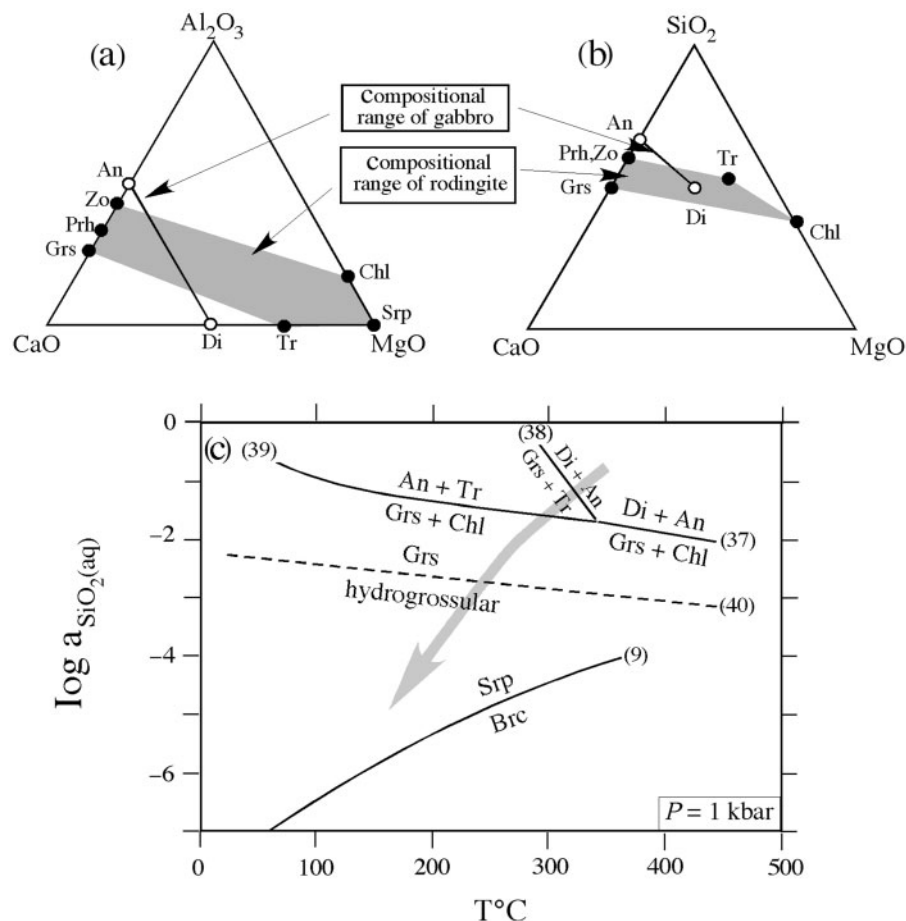


**Fig. 10.** Diagrams showing the chemical changes associated with the formation of rodingites. (a), (b)  $\text{CaO}$ – $\text{Al}_2\text{O}_3$ – $\text{MgO}$  and  $\text{CaO}$ – $\text{SiO}_2$ – $\text{MgO}$  chemographic triangles comparing the assemblages found in gabbro (open circles) with those found in rodingites. It should be noted that rodingites generally have lower silica abundances than the parent gabbro. (c)  $T$ – $\log a_{\text{SiO}_2(\text{aq})}$  diagram showing that the formation of hydrogrossular–chlorite, a common assemblage in rodingites, is accompanied by a decrease in silica activity (gray arrow).

where  $x$  may range up to unity. The thermodynamics of reaction (40) are unconstrained. However, the formation of hydrogrossular obviously involves desilication and hence its occurrence is consistent with the low-Si environment intrinsic to serpentinizing peridotite (Fig. 10c).

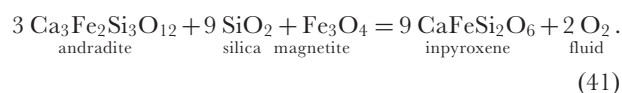
Although silica activity may be the driving force for many rodingite-forming reactions, it is clear from bulk chemistry that elements besides Si, especially Ca, are also mobile (e.g. O'Hanley, 1996). The addition of Ca to rodingites is certainly a consequence of the high Ca content of serpentinizing fluids as discussed above. For rodingites formed from gabbroic rocks, much of the Ca addition probably results from the replacement of Na–Ca plagioclase with Ca-silicates such as grossular or prehnite. In these circumstances, Na is lost to the fluid and/or reprecipitated as Na minerals such as albite, jadeite or analcime, either locally or elsewhere in the hydrothermal system (Whitmarsh *et al.*, 1998; Beard *et al.*, 2002; Li *et al.*, 2004).

## THE OCCURRENCE OF OTHER LOW-SILICA MINERALS IN SERPENTINITES

### Andradite and hydroandradite

Andraditic garnet containing varying amounts of  $\text{Cr}_2\text{O}_3$ ,  $\text{TiO}_2$ , and  $\text{H}_2\text{O}$  has been found in a number of serpentinite parageneses including serpentine–awaruite–andradite  $\pm$  magnetite  $\pm$  brucite (Botto & Morrison, 1976; Onuki *et al.*, 1981; Beard & Hopkinson, 2000), serpentine + diopside + magnetite (Amthauer *et al.*, 1974; Muntener & Hermann, 1994) and serpentine + carbonate + magnetite (Peters, 1965). Evidently it is stable in serpentinites over a range of oxygen fugacities and Ca activities.

Nominally the stability of andradite relative to clinopyroxene is governed by the reaction

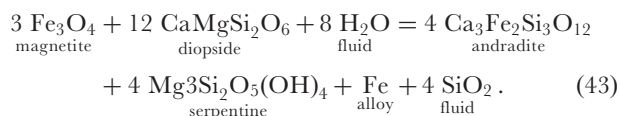
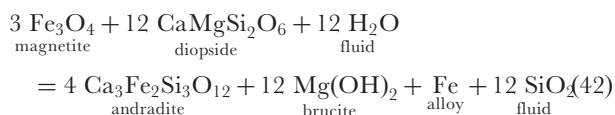


In a silica-saturated system involving pure phases this equilibrium lies between the HM and FMQ buffers; that is, about two log units above FMQ. In a silica-undersaturated system with pure phases, the log of the equilibrium constant for reaction (41) is

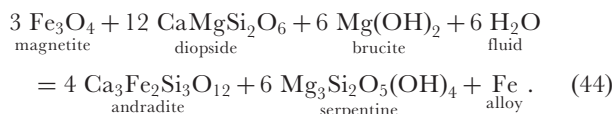
$$\log K_{41} = 2 \log f_{\text{O}_2} - 9 \log a_{\text{SiO}_2}.$$

From this it is evident that the stability of andradite is highly sensitive to silica activity, which explains why, in rocks of low silica activity, such as serpentinites, andradite can be stable even in the presence of native iron (Frost, 1985).

In serpentinites where native iron is dissolved into Fe–Ni alloys (generally awaruite), andradite may form from diopside by the following oxygen-independent reactions (Fig. 11a):



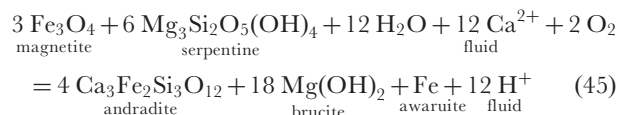
A system that is buffered by the assemblage serpentine–brucite–diopside–magnetite will eventually reach the invariant point marked by the reaction



At this point andradite will become the stable Ca phase in serpentinites. The temperature of this intersection depends on the Ca content and pH of the ambient fluid (because diopside stability is a strong function of these variables, e.g. Fig. 9); for most fluid compositions we used the intersection that lies between 200 and 230°C (Fig. 11a).

If reaction (44) controls the occurrence of andradite in a rock, the resulting assemblages would be Srp–Br–Adr–Di–I or Srp–Br–Adr–Mag–I. The serpentinites from ODP hole 1068A described by Beard & Hopkinson (2000) have the assemblage Srp–Br–Adr–Aw and lack both magnetite and diopside. Although reaction (44) limits the stability of andradite, the assemblage itself must have formed by another process. Beard & Hopkinson (2000) interpreted the serpentinites from hole 1068A as having formed in contact with fluids being expelled from an active serpentinization front at depth. The unusual magnetite-free assemblage Srp–Br–Adr–Aw appears to be related to this fluid flow. Specifically, breakdown of

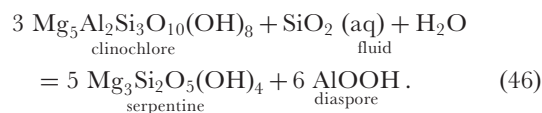
clinopyroxene at depth via reaction (31) yields a high-pH, Ca-rich fluid, which allows the reaction



This leads to the consumption of magnetite in the serpentinite (see Fig. 11b) and may also be responsible for the formation of the Fe-rich brucite [up to 60% Fe(OH)<sub>2</sub> end-member] seen in the hole 1068 rocks (Beard & Hopkinson, 2000). It should be noted that, as for hydrogrossular, hydroandradite should be stable at silica activities lower than those at which andradite proper is stable.

### Diaspore and corundum

Aluminum hydroxide (diaspore and/or gibbsite) occurs in hydrothermally altered submarine serpentinites from the Iberian margin and can occur in other serpentinized peridotites (Beard & Hopkinson, 2000; Kovacs *et al.*, 2002). Diaspore plus brucite can form under extremely low Si activities by desilication of chlorite (Fig. 12). These silica activities, however, also require the desilication of serpentine and are not likely to be regularly attained in serpentinizing peridotite. The surprising presence of diaspore in the Iberian rocks, therefore, is probably a consequence of a second, low-*T* diaspore-forming reaction (see Fig. 12):



Reaction (46) may well be driven by late addition to a serpentinite of silica from seawater. The paradoxical formation of diaspore by a silication reaction reflects the instability of chlorite with respect to saponite clays at low temperature. The presence of diaspore in serpentinites should reflect alteration occurring at *T* < 50°C.

Although corundum never occurs in serpentinites—chlorite is always more stable than serpentine + corundum—it is commonly found in hydrothermally altered rocks associated with metaperidotites (Schreyer *et al.*, 1981; Kerrich *et al.*, 1987; Grapes & Palmer, 1996). Although these rocks have clearly been altered metasomatically sometime in their history, the timing of this metasomatism and, hence the origin of these rocks, is controversial [compare Schreyer *et al.* (1981) and Kerrich *et al.* (1987)]. Recently, Bucher *et al.* (2005) demonstrated that the corundum-bearing rocks probably formed by metasomatic alteration of aluminous metasedimentary rocks adjacent to serpentinite (or metaperidotite). The low silica activity necessary for the formation of corundum is caused by the extraction of silica from these rocks into the adjacent metaperidotite.

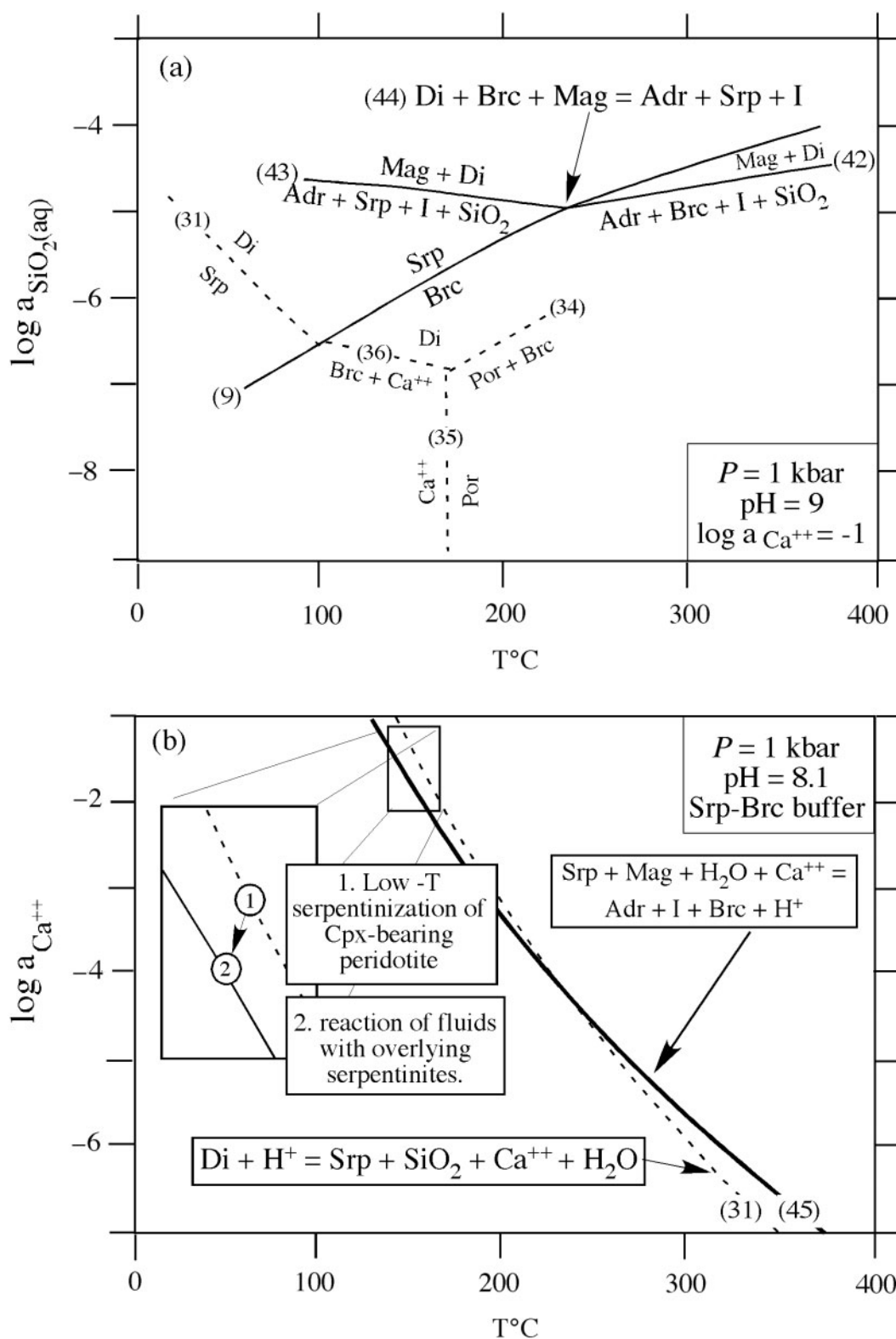


**Fig. 11.** Diagrams showing the stability of andradite in serpentinites. (a)  $\log a_{\text{SiO}_2(\text{aq})}$ – $T$  diagram showing the relations between serpentine, brucite, diopside, magnetite, andradite, and native iron. (b)  $\log a_{\text{Ca}^{++}}$ – $T$  diagram comparing the stability of andradite in serpentinite with that of diopside. Inset shows how the assemblage serpentine + andradite + brucite + iron could form by the reaction between fluids generated from low- $T$  serpentinization of Cpx-bearing peridotite with overlying serpentinite.

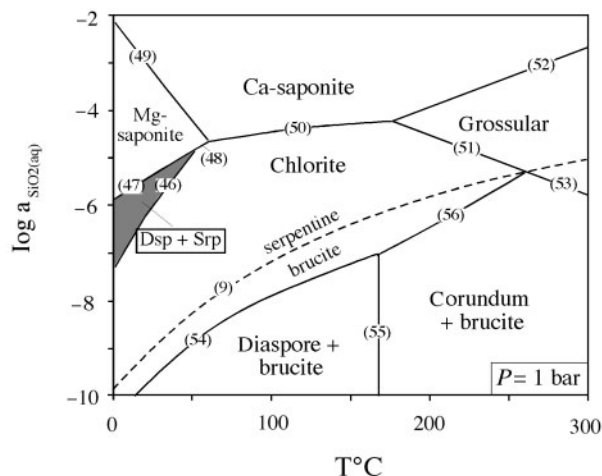


**Fig. 12.**  $\log a_{\text{SiO}_2(\text{aq})}$ - $T$  diagram comparing the stabilities of chlorite, saponite, diaspore, and corundum at 1 bar and in equilibrium with seawater ( $\text{pH}=8.1$ ,  $\log a_{\text{Ca}^{2+}} = -3.75$ ). Shaded area shows a small field for diaspore stability at low  $T$  and relatively high silica activity.

### Jadeite

Although jadeite is a characteristic mineral of high- $P/T$  metamorphic terranes, it is well known that serpentinization plays a key role in the formation in massive jadeite, including all known occurrences of precious jade. Specifically, jadeite forms by crystallization from a Na-rich fluid with a low  $a_{\text{SiO}_2}$  mediated by the presence of actively serpentinizing peridotite (Harlow & Sorensen, 2005). As noted by Harlow & Sorensen (2005), the relationship between jadeite formation and low  $a_{\text{SiO}_2}$  related to serpentinization was anticipated by Coleman (1961). Harlow & Sorensen (2005) noted that quartz is almost unknown in precious jade deposits and that late-stage silicification [analogous to that which occurs under the fluid-dominated conditions in fully serpentinized peridotite (Frost, 1985)] commonly produces rims of albite or other relatively siliceous assemblages around jadeite bodies.

Under even moderately low silica activities, the stability of jadeite is governed by its hydration to analcime [reaction (58)], rather than its reaction to albite + quartz [reaction (57)] (Fig. 13). Figure 13 shows that in these low-silica environments jadeite is stable to lower pressure than it would be in quartz-bearing rocks, but that it still requires moderate pressures (4–6 kbar) to stabilize jadeite relative to analcime. This explains why most jadeite deposits are formed in blueschist terranes and why analcime is present instead in low- $P$  environments (e.g. Whitmarsh *et al.*, 1998).

### DISCUSSION

Recognizing the important role that silica activity plays in serpentinization not only provides petrologists with a conceptual framework to understand the complex

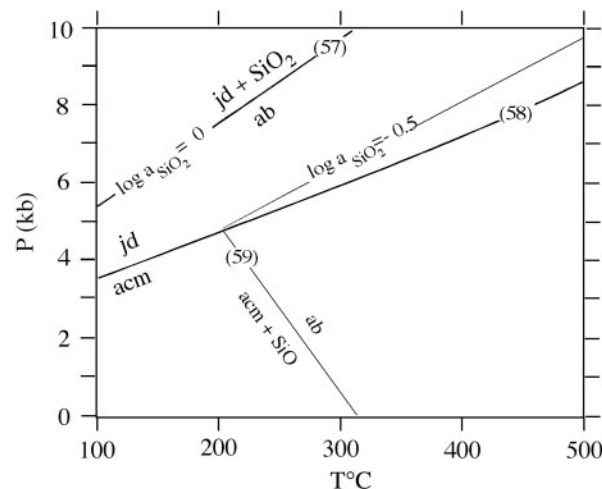


**Fig. 13.**  $P$ - $T$  diagram showing the stabilities of jadeite and analcime relative to albite. (Note how low silica activities stabilize jadeite to lower pressures.)

**Table 6:** *Important accessory minerals in serpentinites*

Mineral	Petrological implications
diopside	most likely to be present in high- $T$ serpentinites, the temperature depends on fluid/rock ratio
andradite	if present with brucite it indicates low- $T$ serpentinization ( $T < 225^\circ\text{C}$ )
diaspore	indicative of very low temperatures (probably $< 100^\circ\text{C}$ ), not compatible with brucite

mineralogical changes that accompany the hydration of peridotite rocks, it also presents us with important tools to unlock the processes that are involved. It provides us with a way to constrain the temperatures at which serpentinization occurs and with a means to characterize the pathways that fluid followed during serpentinization.

We recognize three minerals that may indicate the temperature at which serpentinization occurred (Table 6). The first of these is diopside. The assemblage serpentine (antigorite or lizardite)–brucite–diopside is considered to be indicative of the lowest temperatures of metamorphism (Evans, 1977). Unfortunately, most serpentinites lack diopside because, as temperatures fall, diopside becomes increasingly soluble in serpentinites. Between  $300^\circ\text{C}$  and  $100^\circ\text{C}$  the  $\text{Ca}^{2+}$  activity in the assemblage Di–Srp–Br increases by more than three orders of magnitude (Fig. 9). The occurrence of diopside in a serpentinite, therefore, is a function of both the temperature of serpentinization and the fluid/rock ratio, with diopside being more stable at high  $T$  and low fluid/rock ratios.

As indicated in Fig. 11, andradite in brucite-bearing serpentinites is stable only around 225°C and thus the assemblage andradite–brucite–serpentine may indicate low- $T$  serpentinization. However, the presence of andradite alone in serpentinites is not a temperature indicator, because andradite stability is strongly dependent on silica activity; it may be stable in brucite-free serpentinite at higher  $T$ . Finally, diaspore rarely occurs in serpentinites and its occurrence should indicate very low- $T$  serpentinization. It is also stable only at relatively high silica activity and cannot occur with brucite.

Understanding that silica activity plays an important role in serpentinization provides petrologists with a key to interpreting the textures of serpentinites and, hence, to understanding the process by which a given rock body was hydrated. The assemblage brucite–serpentine controls the low silica activity in serpentinites, but reactions such as the hydration of Opx, the formation of magnetite and the dissolution of diopside contribute silica to the rock that will consume brucite. Therefore, the distribution of Opx and Cpx (or relict Opx and Cpx), magnetite, and brucite within a serpentinite may provide key information about the scale over which silica activity varied within a serpentinite, and this will provide important clues to the process by which serpentinization occurred.

Although it is simple to document the occurrences of Opx, magnetite, and diopside in serpentinites, it is much more difficult to constrain the spatial distribution of brucite. In some serpentinites brucite occurs in relatively large grains (albeit still microscopic) (Beard & Hopkinson, 2000). In others it is either absent or cryptically present as interlayers within serpentine. Petrologists, therefore, cannot assume brucite is absent from a serpentinite even if it is not evident petrographically. Future studies should either use microprobe analyses to identify serpentine–brucite mixtures [as was done by Bach *et al.* (2006)], or use X-ray mapping to find the distribution of brucite in a rock.

The distribution of brucite in a rock is important because it may provide evidence of fluid pathways that operated during serpentinization and may indicate the direction of fluid flow. Fluid that is moving downward, either seawater or fluid that is in equilibrium with gabbro, will have higher silica activity than the assemblage brucite + serpentine. Thus, prolonged downward fluid flow should consume brucite. Fluids in equilibrium with metagabbro may even have high enough silica activity to alter serpentine to talc. Downward-moving fluids, therefore, should move through channels that are brucite-free and, especially near contacts with gabbros, may be talc-bearing. In contrast, fluids that are moving upward from a serpentinization front should have low silica activity and their pathways should be marked by the presence of abundant brucite. If the temperature were

low enough and if the fluids were rich enough in  $\text{Ca}^{2+}$ , their presence may also be marked by the occurrence of andradite (Beard & Hopkinson, 2000).

## CONCLUSIONS

We have shown that the distinctive petrological and geochemical properties of serpentinites—their highly magnetic nature, the reducing conditions, the calcic, high-pH fluids issuing from them—are all tied to the low silica activity of these rocks. The hydration of forsterite to form serpentine and brucite and this reaction's attendant effects on silica activity are ultimately responsible for all these distinctive mineralogical and hydrochemical features. The very low silica activities of the assemblage serpentine–brucite provide the chemical potential needed for virtually all of the geological and mineralogical oddities associated with serpentinization. First, low silica activity lowers the stability of the  $\text{Fe}_3\text{Si}_2\text{O}_5(\text{OH})_4$  component in serpentine, such that some of the ferrous iron in the primary olivine must go into magnetite (in most cases), metallic iron phases, or andradite. The formation of oxidized iron phases, especially magnetite, from the ferrous iron in silicates is the root cause of the characteristically reduced conditions found in serpentinites. A secondary effect of low oxygen fugacity is the reduction of sulfur, leading the stabilization of low-sulfur sulfides (e.g. heazlewoodite) and sulfur-free metal alloys (e.g. awaruite). Second, the instability of clinopyroxene at low silica activity results in its incongruent dissolution, producing the Ca-rich fluids associated with serpentinization. The pH of these fluids is a function of  $T$ , being acidic at high  $T$  but alkaline at the lower temperatures of most serpentinizing systems. Third, many of the unusual minerals that characterize serpentinites (e.g. hydrogarnet and jadeite) are low-Si phases stabilized by low silica activity. Finally, metasomatic processes that accompany serpentinization, including the formation of rodingite and blackwall alteration, are, first and foremost, desilication processes. This observation demonstrates that important geochemical variables, including pH and oxygen fugacity, may be derivative features that are controlled by chemical potentials to which they are only indirectly related.

## ACKNOWLEDGEMENTS

The authors would like to thank the Joint Oceanographic Institutions for allowing us to sail on IODP Expeditions 304 and 305 and providing us access to the samples. Without the chance to interact and puzzle over the formation of serpentinite in Hole U1309D we would never have come up with the insights necessary to write this paper. This work was supported by the grant JOI 48299 to B.R.F. and by the Virginia Museum of Natural History. The authors are particularly thankful for perceptive

reviews by Wolfgang Bach, Bernard Evans, and Richard Laurent, which greatly improved the quality of this paper. Funding to pay the Open Access publication charges for this article was provided by NSF grant EAR 06398980.

## REFERENCES

- Abrajano, T. A., Sturchio, N. C., Bohlke, J. K., Lyon, G. L., Poreda, R. J. & Stevens, C. M. (1988). Methane–hydrogen seeps, Zambales Ophiolite, Philippines: Deep or shallow origin? *Chemical Geology* **71**, 211–222.
- Allen, D. E. & Seyfried, W. E. (2003). Compositional controls on vent fluids from ultramafic-hosted hydrothermal systems at midocean ridges: An experimental study at 400°C, 500 bars. *Geochimica et Cosmochimica Acta* **67**, 1531–1542.
- Amthauer, G., Kurtz, W., Rost, F. & Schloemer, H. (1974). Chemismus und Genese des Andradits aus dem Serpentin des Val Malenco Schweiz. *Mineralogische und Petrographische Mitteilungen* **54**, 691–706.
- Andersen, D. J., Lindsley, D. H. & Davidson, P. M. (1993). QUILF: A PASCAL program to assess equilibria among Fe, Mg, Mn, Ti oxides, pyroxenes, olivine, and quartz. *Computers and Geosciences* **19**, 1333–1350.
- Bach, W., Paulick, H., Garrido, C. J., Ildefonse, B., Meurer, W. P. & Humphris, S. E. (2006). Unraveling the sequence of serpentinization reactions: petrography, mineral chemistry and petrophysics of serpentinites from MAR 15°N (ODP Leg 209, Site 1274). *Geophysical Research Letters* **33**, L13306, doi:10.1029/2006GL025681.
- Barnes, I. & O'Neil, J. R. (1969). The relationship between fluids in some fresh alpine-type ultramafics and possible modern serpentinization. *Geological Society of America Bulletin* **80**, 1947–1960.
- Barnes, I., O'Neil, J. R. & Trescases, J. J. (1978). Present day serpentinization in New Caledonia, Oman, and Yugoslavia. *Geochimica et Cosmochimica Acta* **42**, 144–145.
- Beard, J. S. & Hopkinson, L. (2000). A fossil, serpentinization-related hydrothermal vent, Ocean Drilling Program Leg 173, Site 1068 (Iberia Abyssal Plain): Some aspects of mineral and fluid chemistry. *Journal of Geophysical Research* **105**, 16527–16540.
- Beard, J. S., Fullagar, P. D. & Sinha, A. K. (2002). Gabbroic pegmatite intrusions, Iberia Abyssal Plain, ODP leg 173, Site 1070: Magmatism during a transition from non-volcanic rifting to seafloor spreading. *Journal of Petrology* **43**, 885–905.
- Bethke, C. M. (2005). *The Geochemists Workbench®, Version 6.0, GWB Essentials Guide*. Urbana, IL: Hydrogeology Program, University of Illinois, 76 pp.
- Botto, R. I. & Morrison, G. H. (1976). Josephinite: a unique nickel–iron. *American Journal of Science* **276**, 241–274.
- Bucher, K., De Capitani, C. & Grapes, R. (2005). The development of a margarite–corundum blackwall by metasomatic alteration of a slice of mica schist in ultramafic rocks, Kvesölen, Norwegian Caledonides. *Canadian Mineralogist* **43**, 129–156.
- Carmichael, I. S., Turner, F. J. & Verhoogen, J. (1974). *Igneous Petrology*. New York: McGraw–Hill.
- Chamberlain, J. A., McLeod, C. R., Traill, R. J. & Lachance, G. R. (1965). Native metals in the Muskox intrusion. *Canadian Journal of Earth Sciences* **2**, 188–215.
- Charlou, J. L., Fouquet, Y., Bougault, H., Donval, J. P., Etoubleau, J., Jean-Baptiste, P., Dapigny, A., Appriou, P. & Rona, P. A. (1998). Intense CH<sub>4</sub> plumes generated by serpentinization of ultramafic rocks at the intersection of the 15°20'N fracture zone and the Mid-Atlantic Ridge. *Geochimica et Cosmochimica Acta* **62**, 2323–2333.
- Charlou, J. L., Donval, J. P., Fouquet, Y., Jean-Baptiste, P. & Holm, N. (2002). Geochemistry of high H<sub>2</sub> and CH<sub>4</sub> vent fluids issuing from ultramafic rocks at the Rainbow hydrothermal field, (36°14'N, MAR). *Chemical Geology* **191**, 345–359.
- Coleman, R. G. (1961). Jadeite deposits of the Clear Creek area, New Idria district, San Benito County, California. *Journal of Petrology* **2**, 209–247.
- Coleman, R. G. (1963). *Serpentinites, Rodingites, and Tectonic Inclusions in Alpine-type Mountain Chains*. Geological Society of America, *Special Papers* **73**.
- Coleman, R. G. (1971). Petrologic and geophysical nature of serpentinites. *Geological Society of America Bulletin* **82**, 897–918.
- Coleman, R. G. (1977). *Ophiolites, Ancient Oceanic Lithosphere?* Berlin: Springer.
- Eckstrand, O. R. (1975). The Dumont serpentinite: a model for control of nickeliferous opaque mineral assemblages by alteration reactions in ultramafic rocks. *Economic Geology* **70**, 183–201.
- El-Shazly, A. K. & Al-Belushi, M. (2004). Petrology and chemistry of metasomatic blocks from Bawshir, northeastern Oman. *International Geology Review* **46**, 904–938.
- Evans, B. W. (1977). Metamorphism of alpine peridotite and serpentinite. *Annual Review of Earth and Planetary Sciences* **5**, 397–447.
- Evans, B. W. (2004). The serpentinite multisystem revisited; chrysotile is metastable. *International Geology Review* **46**, 479–506.
- Evans, B. W. & Frost, B. R. (1975). Chrome-spinel in progressive metamorphism—a preliminary analysis. *Geochimica et Cosmochimica Acta* **39**, 959–972.
- Evans, B. W., Trommsdorff, V. & Richter, W. (1979). Petrology of an eclogite–metarodinite suite at Cima di Gagnone, Ticino, Switzerland. *American Mineralogist* **64**, 15–31.
- Frost, B. R. (1975). Contact metamorphism of serpentinite, chloritic blackwall, and rodingite at Paddy-Go-Easy-Pass, Central Cascades, Washington. *Journal of Petrology* **16**, 272–313.
- Frost, B. R. (1985). On the stability of sulfides, oxides, and native metals in serpentinite. *Journal of Petrology* **26**, 31–63.
- Frost, B. R., Beard, J. S., Abratis, M. W., Andreani, M., Delacour, A., Drouin, M., Fryer, P., McCaig, A., Nozaka, T., Ohara, Y. & the shipboard scientific parties of IODP expeditions 304 and 305 (2005). Importance of silica activity to the serpentinization processes: Insights from microrodinites in IODP hole U1309D. EOS Transactions of the American Geophysical Union, Abstract V51B-1483.
- Grapes, R. & Palmer, K. (1996). (Ruby–sapphire)–chromian mica–tourmaline rocks from Westland, New Zealand. *Journal of Petrology* **37**, 293–315.
- Groves, D. J. & Keays, R. R. (1979). Mobilization of ore-forming elements during alteration of dunites, Mt. Keith–Betheno, Western Australia. *Canadian Mineralogist* **17**, 373–389.
- Harlow, G. E. & Sorensen, S. S. (2005). Jade (nephrite and jadeite) and serpentinite: Metasomatic connections. *International Geology Review* **47**, 116–146.
- Holland, T. J. B. & Powell, R. (1998). An internally consistent thermodynamic dataset for phases of petrologic interest. *Journal of Metamorphic Geology* **16**, 309–343.
- Johnson, J. W., Oelkers, E. H. & Helgeson, H. C. (1992). SUPCRT92: A software package for calculating the standard molal thermodynamic properties of minerals, gases, aqueous species, and reactions from 1 to 5000 bar and 0 to 1000°C. *Computers and Geosciences* **18**, 899–947.
- Kelley, D. S., Karson, J. A., Blackman, D. K., Früh-Green, G. L., Butterfield, D. A., Lilley, M. D., Olson, E. J., Schrenk, M. O., Roe, K. K., Lebon, G. T. & Rivizzigno, P. (2001). An off-axis

- hydrothermal vent field near the Mid-Atlantic Ridge at 30. *Nature* **412**, 145–149.
- Kelley, D. S., Karson, J. A., Früh-Green, G. L., Yoerger, D. R., Shank, T. M., Butterfield, D. A., Hayes, J. M., Schrenk, M. O., Olson, E. J., Proskurowski, G., Jakuba, M., Bradley, A., Larson, B., Ludwig, K., Glickson, D., Buckman, K., Bradley, A. S., Brazelton, W. J., Roe, K., Elend, M. J., Delacour, A., Bernasconi, S. M., Lilley, M. D., Baross, J. A., Summons, R. E. & Sylva, S. P. (2005). A serpentinite-hosted ecosystem; the Lost City hydrothermal field. *Science* **307**, 1428–1434.
- Kerrick, R., Fyfe, W. S., Barrett, R. L., Blair, B. B. & Willmore, L. M. (1987). Corundum, Cr-muscovite rocks at O'Briens, Zimbabwe: the conjunction of hydrothermal desilification and LIL-element enrichment—geochemical and isotopic evidence. *Contributions to Mineralogy and Petrology* **95**, 481–498.
- Kovacs, G., Raucsik, B. & Horváth, P. (2002). Mineral composition of the Gyöd serpentinite body, southern Transdanubia, Hungary. *Acta Mineralogica–Petrographica* **43**, 71–77.
- Leblanc, M. & Lbouabi, M. (1988). Native silver mineralization along a rodingite tectonic contact between serpentinite and quartz diorite (Bou Azzer, Morocco). *Economic Geology* **83**, 1379–1391.
- Le Gleuher, M., Livi, K. J. T., Veblen, D. R., Noack, Y. & Amouric, M. (1990). Serpentinization of enstatite from Pernes, France: Reaction microstructures and the role of system openness. *American Mineralogist* **75**, 813–824.
- Li, X.-P., Rahn, M. & Bucher, K. (2004). Metamorphic processes in rodingites of the Zermatt–Saas ophiolites. *International Geology Review* **46**, 28–51.
- Muntener, O. & Hermann, J. (1994). Titanian andradite in a metapyroxenite layer from the Malenco ultramafics (Italy): implications for Ti-mobility and low oxygen fugacity. *Contributions to Mineralogy and Petrology* **116**, 156–168.
- O'Hanley, D. S. (1996). *Serpentinites: Records of Tectonic and Petrological History*. Oxford Monographs on Geology and Geophysics **34**, 277p.
- O'Hanley, D. S., Schandl, E. S. & Wicks, F. J. (1992). The origin of rodingites from Cassiar, British Columbia and their use to estimate *T* and *P*(H<sub>2</sub>O) during serpentinization. *Geochimica et Cosmochimica Acta* **56**, 97–108.
- Onuki, H., Yoshida, T. & Nodachi, M. (1981). Notes on petrography and rock-forming mineralogy: X. Awaruite and other accessory minerals coexisting with Ti-rich hydroandradite in metamorphosed ultramafics of the Sanbagawa belt. *Journal of the Japanese Association of Mineralogists, Petrologists, and Economic Geologists* **76**, 372–375.
- Oufi, O., Cannat, M. & Horen, H. (2002). Magnetic properties of variably serpentinized abyssal peridotites. *Journal of Geophysical Research* **107**, doi:10.1029/2001JB000549.
- Palandri, J. L. & Reed, M. H. (2004). Geochemical models of metasomatism in ultramafic systems: Serpentinization, rodingitization, and sea floor carbonate chimney precipitation. *Geochimica et Cosmochimica Acta* **68**, 1115–1133.
- Peretti, A., Dubessy, J., Mullis, J., Frost, B. R. & Trommsdorff, V. (1992). Highly reducing conditions during Alpine metamorphism of the Malenco peridotite (Sondrio, northern Italy) indicated by mineral paragenesis and H<sub>2</sub> in fluid inclusions. *Contributions to Mineralogy and Petrology* **112**, 329–340.
- Peters, T. (1965). A water-bearing andradite from the Totalp serpentinite (Davos, Switzerland). *American Mineralogist* **50**, 1482–1486.
- Puga, E., Nieto, J. M., Diaz de Federico, A., Bodinier, J. L. & Morten, L. (1999). Petrology and metamorphic evolution of ultramafic rocks and dolerite dykes of the Betic ophiolitic association (Mulhacen Complex, SE Spain): evidence of eo-Alpine subduction following an ocean-floor metasomatic process. *Lithos* **49**, 23–56.
- Ramdohr, P. (1968). *Ore Minerals and their Intergrowths*. Oxford: Pergamon.
- Rosetti, P. & Zuchetti, S. (1998). Occurrence of native iron, Fe–Co and Ni–Fe alloys in the serpentinite from the Balangero asbestos mine (Western Italian Alps). *Ophioliti* **13**, 43–56.
- Russell, M. J. & Arndt, N. T. (2005). Geodynamic and metabolic cycles in the Hadean. *Biogeosciences* **2**, 97–111.
- Russell, M. J. & Hall, A. J. (1997). The emergence of life from iron monosulphide bubbles at a submarine hydrothermal redox and pH front. *Journal of the Geological Society, London* **154**, 377–402.
- Schandl, E. S., O'Hanley, D. S. & Wicks, F. J. (1989). Rodingites in serpentinized ultramafic rocks of the Abitibi greenstone belt, Ontario. *Canadian Mineralogist* **27**, 579–591.
- Schreyer, W., Werding, C. & Abraham, K. (1981). Corundum–fuchsite rocks in greenstone belts of Southern Africa: petrology, geochemistry and possible origin. *Journal of Petrology* **22**, 191–231.
- Schroeder, T., John, B. & Frost, B. R. (2002). Geologic implications of seawater circulation through peridotite exposed at slow-spreading mid-ocean ridges. *Geology* **30**, 367–370.
- Shervais, J. W., Kolesar, P. & Andreasen, K. (2005). A field and chemical study of serpentinization—Stonyford, California: chemical flux and mass balance. *International Geology Review* **47**, 1–28.
- Shive, P. N., Frost, B. R. & Peretti, A. (1988). The magnetic properties of metaperidotitic rocks as a function of metamorphic grade: implications for crustal magnetic anomalies. *Journal of Geophysical Research* **93**, 12187–12195.
- Sleep, N. H., Meibom, A., Fridriksson, Th., Coleman, R. G. & Bird, D. K. (2004). H<sub>2</sub>-rich fluids from serpentinization: Geochemical and biotic implications. *Proceedings of the National Academy of Sciences of the USA* **101**, 12818–12823.
- Toft, P. B., Arkanai-Hamed, J. & Haggerty, S. E. (1990). The effects of serpentinization on density and magnetic susceptibility: a petrophysical model. *Physics of the Earth and Planetary Interiors* **65**, 137–157.
- Trommsdorff, V. & Evans, B. W. (1972). Progressive metamorphism of antigorite schist in the Bergell tonalite aureole (Italy). *American Journal of Science* **272**, 423–437.
- Viti, C., Mellini, M. & Rumori, C. (2005). Exsolution and hydration of pyroxenes from partially serpentinized harzburgites. *Mineralogical Magazine* **69**, 491–507.
- Whitmarsh, R. B., Beslier, M.-O. & Wallace, P. & the Leg 173 Shipboard Scientific Party (1998). Sites 1065–1070, Iberia Abyssal Plain. In: Whitmarsh, R. B., Beslier, M.-O. & Wallace, P. J. *et al.* (eds) *Proceedings of the Ocean Drilling Program, Initial Reports*, 173. College Station, TX: Ocean Drilling Program.
- Yoder, H. S., Jr & Tilley, C. E. (1962). Origin of basalt magmas: An experimental study of natural and synthetic rock systems. *Journal of Petrology* **3**, 342–532.